Understanding site formation processes, human occupation and environmental change at Mertenhof rock shelter, South Africa

Alanah Bainbridge
Bachelor of Archaeology

Thesis
Submitted to Flinders University
for the degree of

Masters of Archaeology and Heritage Management

Flinders University

7/08/2023

TABLE OF CONTENTS

ABSTRACT

This thesis explores the sedimentary properties of Mertenhof rock shelter, situated in South Africa. Methods including particle size and shape, magnetic susceptibility, loss on ignition and elemental analysis provided more information about the climate mechanisms operating over a period of >150 ka. The results showed how these events affected the formation of the site. The analysis identified that Mertenhof's deposition history was impacted by at least three large scale climate events that contributed to the formation of the site. These climate events – the last glacial maximum (LGM), LGM/Marine Isotope Stage (MIS) 3 transition, MIS 3/4 transition, MIS 5 and possibly MIS 6 – register at Mertenhof as small oscillations in the grain size and magnetic susceptibility results. For example, the LGM is defined by finer grained sediment that is associated with the onset of aeolian deposition, as supported in the regions paleoenvironmental data. Fine grains are replaced by coarser sediment during later MIS 3, linked with cool and wet conditions and the onset of internal erosion. A peak in magnetic susceptibility (interpreted here as anthropogenically induced) during MIS 3 supports the findings of Williams (2017) and reiterates that Mertenhof was occupied during this time. The MIS 3/4 transition is marked by a decline in magnetic susceptibility values, describing a period of harsh glacial conditions during MIS 4 that increased the percentage of internal erosion.

DECLARATION

I certify that this thesis:

1. does not incorporate without acknowledgment any material previously submitted for a degree or diploma in any university

2. and the research within will not be submitted for any other future degree or diploma without the permission of Flinders University; and

3. to the best of my knowledge and belief, does not contain any material previously published or written by another person except where due reference is made in the text.

Signed: Alanah Bainbridge

Date: 7/08/2023

ACKNOWLEDGEMENTS

Firstly, I would like to thank my supervisor Ian Moffat for his support and guidance during this process. The knowledge I have learnt from you and from completing this thesis is invaluable to me, and I thank you for your patience and willingness to help me through this. I would also like to thank Rachel Rudd for her help and endless patience in the laboratory, if it wasn't for her I'm sure my experience in the lab would not have run so smoothly. Also, Alex Mackay for providing me with the information on Mertenhof that I needed to complete this thesis.

Last but not least, I would also like to thank my family, especially my Mum, Dad and Pa for their love and support in this journey. Also the friends (you know who you are) who helped me, not only during this thesis but throughout this entire degree, you guys have played a big part in my success over these 6 years. It certainly was a long journey, but I am grateful for everyone who played a part in helping me achieve my goals of becoming an archaeologist.

LIST OF FIGURES

LIST OF TABLES

CHAPTER ONE: INTRODUCTION

1.1 Introduction

An understanding that the relationship between past humans and their environments was neither directional nor consistent is vital to piecing together the past. It is important to recognise climate as a major component in the sedimentary makeup of a site, not only because of the geological impacts (for example preservation issues and the introduction/removal of sediment by weather), but because of the potential effects on human behaviour (French 2003; Goldberg and Macphail 2006; Hassen 1979; Shahack-Gross 2017; Waters and Kuehn 1996). Early humans were forced to modify their living arrangements, technology, and culture to adapt to their changing surroundings. Therefore to understand why humans reacted a certain way it is important to understand the primary mechanisms that were driving these reactions to begin with.

The study of site formation is significant because the archaeology of a site is contained within the sediments. Investigating the structure of site formation and any geological, human, or other (e.g., animal) processes which may impact the preservation or formation of this record is needed to fully understand a sites depositional and archaeological history (Arroyo-Kalin 2020:426; Barham and Huckleberry 2014:49; Hassen 1979:267; Waters and Kuehn 1996:494). Understanding the stratigraphy allows a comprehensive understanding of, for example, dates, sediment accumulation rate, and erosion events.

While the extent of these processes operates on a case-to-case basis, the ability to predict human movement and behaviour relies heavily on archaeologist's understanding of the geological processes which have most certainly impacted the sedimentary-profile of the archaeological record (Waters and Kuehn 1996:495), and the climate conditions that have affected behaviour.

While evidence of human adaptions to climate change was experienced globally (e.g., Levin 2015; Timmermann and Friedrich 2016; Williams et al. 2015), South Africa holds an important place within the context of human transmission and dispersal. The southwestern Cape of South Africa was affected by an extreme level of climate variability that forced early humans to make behavioural and occupational modifications to adapt to their changing surroundings. Unfortunately, the South African archaeological record is hindered by poor resolution of occupation and technological transmission, and significant climate variability (Mackay et al. 2020).

1.1.1 Climate

The various MIS stages can be divided into 5 stages. They can be described briefly as follows: 5d–5a experienced several fluctuations between colder stadials and warmer interstadials (Henshilwood 2008:7). The cold stadial conditions increased during MIS 4–3 characterised by a brief increase in warm interstadial conditions. MIS 2 falls within the cool glacial conditions of the

LGM, followed by the warm interglacial conditions of the Holocene during MIS 1 (Henshilwood 2008:7).

1.2 Research Aims

This research will explore the sedimentological context of Mertenhof to identify the environmental mechanisms that affected the formation of the site. The analysis will incorporate a wide range of geoarchaeological techniques to reconstruct the climate over the last >150 ka by recognising changes in sediment characteristics. The analysis aims to determine the depositional history of the sediment; whether sediment was deposited by internal mechanisms (e.g., erosion) or introduced externally (e.g., environmental processes such as wind/water), and if factors such as site location had an impact on the process of formation.

The main research aim is: *Understanding site formation processes, human occupation and environmental change at Mertenhof rock shelter, South Africa.* This will be answered by applying geoarchaeological laboratory methods to sediment collected from the site. The methods will include particle size and shape analyses, loss on ignition (LOI), ICP-elemental analysis and lab-based magnetic susceptibility (MS). The results will be used in conjunction with regional paleoenvironmental-proxies to gather a general understanding of the environmental mechanisms at play for the wider region.

Supplementary questions include:

- What do the sedimentary properties of Mertenhof reveal about the paleoenvironment during the Late Pleistocene?
- Are the results of this analysis consistent with other paleoenvironmental data for the region?
- What impact has climate had on sedimentation in Mertenhof rock shelter?
- Is there a clear distinction between archaeological and geological deposits in the results?
- Does the data support occupation at Mertenhof during MIS 3?

1.3 Significance

The site location provides a rare chance to study a deep and stable stratigraphic record for a shelter that is in a geographically and archaeologically significant area. The accumulation of a relatively stable site formation provides a unique geomorphological context to explore regional paleoenvironmental change over a substantial period. The study will contribute to a more detailed understanding of the archaeology of the Karoo Biome, a unique geological area that has a rich and complex archaeological record.

1.4 Thesis Outline

Chapter Two is dedicated to background information on South Africa and the study area. The start of the chapter gives a brief introduction into South African archaeology to provide a full understanding of the country's rich archaeological record, and how this record displays a continuous sequence from the beginnings of humankind right through to modern times. Next, it provides a brief introduction into the Western Cape region. This includes basic information on the geology, climate and hydrology to provide context into the general study area. A review of significant archaeological sites for the region is included to show the importance of the area. A few examples detailing the history of the geoarchaeological work in the region is included to show how these methods have already contributed to the archaeological record of the Western Cape. A climate history spanning from MIS 5 to the present is included next. This section is important to the interpretation and discussion of this analysis and will be referred back to throughout this thesis. The timeline is constructed using environmental evidence from archaeological sites around the Western Cape region and individual paleo-histories. The next section is exclusively focused on Mertenhof, offering basic site information and climate, vegetation and hydrology for the immediate vicinity, and previous research conducted at the site. Past studies at Mertenhof have already shown that the site is unique to Western Cape archaeology, so this section aims to demonstrate the significance of the site, while also acknowledging the value of this study to the local/regional archaeological record; and how an understanding of climate patterns may refine/contribute knowledge regarding the behaviour observed from these past studies.

In Chapter Three, the laboratory methods used in this analysis are discussed in detail. This section is also used to show the suitability of the methods in answering the studies main aim.

Chapter Four presents the results for the laboratory methods conducted on sediment from squares 4 and 6 from the 2017 excavation.

Chapter Five is dedicated to an in-depth discussion on the results. It provides insight into the climate mechanisms operating during the last >150 ka.

Chapter Six addresses possible recommendations for future work and concludes the study.

CHAPTER TWO: BACKGROUND

2.1 The South African archaeological record

South Africa has one of the longest and richest archaeological records in the world (Hall 1996; Mitchell 2002). Encompassing 3,000,000 km2, South Africa has been occupied by early hominin species for nearly 3 million years (Lombard et al. 2012; Mitchell 2002). Along with a diverse geological, ecological, and environmental background, this history of human occupation has created an opportunity to study a large portion of human evolution and technological achievement. This wide and unique diversity means that Southern Africa is at the fore front of major debates, and further research endeavours will undoubtedly increase our knowledge on the beginnings of humankind. The South African hominin record has already produced the largest findings of *Australopithecine* specimens, such as those found at Sterkfontein Caves (Clarke 2008; Clarke 2013; Mitchell 2002). The Drimolen Main Quarry is South Africa's best dated hominin site and yields the oldest known specimen of Early Pleistocene *Homo*, dating to ~2.04 million to 1.95 million years ago, and the oldest lithic assemblages in South Africa (Herries et al. 2020). The findings confirmed that *Australopithecine, Paranthropus,* and early *Homo* species once co-existed around 2 million years ago. These sites are just two examples of South Africa's early archaeological heritage and showcases just how important the country is to the earliest areas of human prehistory. South Africa's archaeological record is split into various archaeological technocomplexes that are listed in Table 1 with the associated geological period.

Early hominin behavioural adaption and evolution is not the only benefit to South Africa's rich archaeological history. A large emphasis has been placed on technocomplexes such as the Pre-Still Bay (pre-SB), Still Bay (SB), Howiesons Poort (HP) and Post-Howiesons Poort (post-HP) (see section 3.2 for further information) from Middle Stone Age (MSA) sites. Investigation of the MSA and the associated technocomplexes is important for understanding modern and archaic *Homo* sapiens. Important sites include Bushman (Badenhorst and Plug 2012), Rose Cottage Cave (Wadley 2001), Duinefontein (Klein et al. 1999), Diepkloof (Miller et al. 2013; Tribolo et al. 2013), and Klasies River Mouth (Butzer 1978). These MSA and related technocomplexes are essential in the debate regarding human cognition, migration patterns outside of Africa, evolution. As well as provide a description into how modern humans adapted to challenges such as climate change. Included in the South African archaeological record is a rich inference of upper/late Pleistocene and Holocene technology. South Africa provides a continuous archaeological record that spans from the very beginnings of human linage, right through to the modern times. As such the country is essential to uncovering the human past.

Pleistocene – 2.6 ma –

Geological Period	Archaeological Period	Technocomplex
Early/Lower Pleistocene (2.6-0.8 ma)	**Earlier Stone Age** (2 ma-200 ka)	**Oldowan** (~2-1.5 ma) **Acheulean** (~1.5 ma-300 ka)
Middle Pleistocene (0.8 ma-125 ka)		**Earlier Stone Age–Middle Stone Age transition** (600-200 ka)
Late/Upper Pleistocene (125-12 ka)	**Middle Stone Age** (300-20 ka)	**Pre-Still Bay** (~96-72 ka) **Still Bay** (~77-70 ka) **Howiesons Poort** (66-58 ka) **Post-Howiesons Poort/Sibudu** (~58-45 ka)
	Later Stone Age (< 40 ka)	**Final Middle Stone Age** (~40-20 ka) **Earlier Later Stone Age** (40-18 ka)
LGM (24-18 ka)		**Robberg** (~ 18-12 ka)
Holocene (12 ka–Present)		**Oakhurst** (~12-7 ka) **Wilton** (~8-4 ka) **final Later Stone Age** (~4-0.1 ka) **ceramic final Later Stone Age** (< 2 ka)

Table 1 Timeline of the technocomplex's within the South African sequence coupled with the correlating geological epochs. Dates for the technocomplexes are based on Dusseldorp et al. (2013)'s review of South Africa's Stone Age, dates for the geological epochs sourced from Bellwood and Ness (2014).

2.2 Background to the Western Cape and the Winter Rainfall Zone

The Western Cape archaeological record was once hindered by minimal archaeological interest, impacting researchers' ability to investigate and reconstruct the prehistory of the area (Chase and Meadows 2007). Recent interest in archaeology (Miller et al. 2013; Low et al. 2017; Mackay et al. 2019), environmental and climate processes (Baxter and Parkington 1996; Stagerr et al. 2012), and vegetation (Meadows and Sugden 1991a; Meadows and Sugden 1991b; Meadows and Sugden 1993), have contributed to a growing body of literature that has refined the area's paleo-history into a fairly comprehensive understanding of archaeological and environmental processes. This record is not complete, but emphasis is being placed on the archaeological significance of the area and its detailed record of human behaviour and occupation patterns. The connection between intense climate fluctuations and human behaviour also furthers the need for combined environmental and archaeological research.

2.2.1 WRZ weather systems

Based on precipitation patterns, South Africa is divided into three main climate zones – the year-round rainfall zone (YRZ), summer rainfall zone (SRZ) and the winter rainfall zone (WRZ) (Mackay et al. 2018:14). The Western Cape is situated in the WRZ towards the southwestern region of South Africa (Mackay et al. 2018:14). The area contains a diverse range of vegetation and lithology and spans from southwestern Namibia to Cape Agulhas, and inland to the west of the Great Escarpment (Ames et al. 2020:2a; Chase and Meadows 2007:104; Weldeab et al. 2013:2348).

The zone experiences seasonal escalation and, during the winter months, the associated northward expansion of the westerlies that controls annual precipitation (Chase et al. 2015:139; Mackay et al. 2018:14). While the circumstances affecting precipitation in the winter months are complex, the majority of evidence supports the theory that precipitation was, and still is, controlled by the expansion of Antarctic Sea ice throughout the late Quaternary (Chase and Meadows 2007; Mackay et al. 2018:14). This expansion is predicted to affect the length and intensity of precipitation and trade wind strength during glacial periods, consequently intensifying regional humidity (Mackay et al. 2018:14; Stuut et al. 2002). The glacial periods during MIS 4 and 2 follow this pattern. Interglacial conditions are expected to be arid and less windy in comparison (Stuut et al. 2002). Understanding the extent of these mechanisms on WRZ paleoclimates may contribute to South Africa's climate record on regional and hemispheric levels (Chase and Meadows 2007).

2.2.2 Geology

The Cederberg region is dominated by two geological supergroups: the Cape Supergroup and younger Karoo Supergroup (Low and Mackay 2018:174). The Cape Supergroup is comprised of

Table Mountain, Bokkeveld and Witteberg Series units and the Karoo Supergroup the Dwyka, Beaufort and Ecca Series, but a dominance of sedimentary rocks belonging to the Table Mountain Series is prevalent (Low and Mackay 2018:174; Schmidt and Mackay 2016:3). These units appear in the form of massive sandstone, shale and quartzite outcrops (Low and Mackay 2018:174). Quartz, a common material used for the manufacture of stone tools, occurs most regularly as pebbles in combination with Table Mountain and Nardouw bed formations and occasionally as veins in the sandstone (Low and Mackay 2018:174).

Hornfels outcrops are absent to the west of the Doring, although sources do occur alongside diabase dykes with Karoo supergroup lithology (Low and Mackay 2018:174; Schmidt and Mackay 2016:5; Shaw et al. 2019:404). The large quantity of geological material means the Doring river played an important role for stone artifact production (Ames et al. 2020b; Low et al. 2017; Mackay et al. 2020; Shaw et al. 2019)

2.2.3 Significance of the Western Cape to the archaeological record

The Western Cape occupies a valuable position within the archaeological record for the study of behaviour, evolution, and transmission of early modern humans. The region contributes an archaeological record that extends back to the Late Pleistocene (Ames et al. 2020b; Low and Mackay 2018; Mackay et al. 2014; Mackay et al. 2015), and recent interest has demonstrated the wealth and significance of such a long and continuous archaeological record to South African history. The region is defined by an infrequent yet repetitive occupation sequence, a rich evolution of technological advancement, and a continuous accumulation of archaeological material spanning across a significant time-period.

Of particular interest is the Western Cape's rich history of SB and HP technocomplexes. These technocomplexes occupy a vital position within the study of early modern human behaviour and behavioural modernity, the complexity of late Pleistocene technology, and the expansion of anatomically modern humans outside of Africa (Deacon 1995; Jacobs et al. 2008; Mackay 2011; McCall and Thomas 2012).

With reference to the HP, the appearance, and its subsequent replacement by less advanced MSA industries have become a point of serious debate regarding early modern human behaviour (Mackay 2011:1431; Wadley 2001:203). The HP appeared around 80-70 ka and contained backed blade technology that was more sophisticated than anything previously seen for the MSA (Mackay 2011:1431; Wadley 2001:203). Further archaeological investigation revealed this level of advancement did not continue into the following MSA industries, and that post-HP technology had more in common with earlier MSA industries.

As such, the HP has been argued to represent the early hallmarks of behavioural modernity (e.g., Deacon 1995; Wurz 1999) because of their association with early symbology and unique stone tool production (Jacobs et al. 2008; Mackay 2011; McCall and Thomas 2012). Some have chosen to disregard the possibility of this industry reflecting the beginnings of cultural modernity, instead arguing in favour of an environmental adaption to MIS 4 (Ambrose and Lorenz 1990; Villa et al. 2010). And another theory: an increase in population that allowed the creation of a new era of advanced technology, as argued by Jacobs et al. (2008). A decrease in population would explain why the industry is not replicated in both earlier and later MSA technologies. It remains to be seen the reason behind the appearance and disappearance of these technologies, but the Western Cape will remain at the front of this debate, and continue to supply wealth to the archaeological record as new sites are studied.

Key rock shelters and open-air localities in the Western Cape include Diepkloof (Miller et al. 2013), Klipfonteinrand rock shelter (Mackay et al. 2020), Klein Kliphuis (Mackay 2010), Putslaagte 8 (Mackay et al. 2015), and Elands Bay (Figure 1) (Porraz et al. 2016).

Figure removed due to copyright restriction

Figure 1 Map of key archaeological sites within the WRZ. EB = Elands Bay, DPK = Diepkloof, KK = Klein Kliphuis, KFR = Klipfonteinrand, MRS = Mertenhof rock shelter, PL8 = Putslaagte 8. Based on data from Ames et al. 2020.

2.2.4 Diepkloof rock Shelter

Diepkloof occupies a unique position in the Western Cape archaeological record because it is one of a few sites with a continuous Late Pleistocene occupation sequence. Previous studies have suggested a relatively detailed occupation sequence between MIS 5 to 3 (Miller et al. 2013:3433). The site is ca. 180 km north of Cape Town on the western coast (Figure 1) Human activity, such as burning, hearth construction and trampling of the surface sediment were identified as the primary influence on the site's formation. A micromorphological analysis (the study of sediment under the microscope) concluded that the sites sedimentary complexity largely resulted from changes in human activity conducted over the site's occupation period (Miller et al. 2013). The site is not consistent with multiple occupation hiatuses (just one instance between the late MSA and early LSA) (Miller et al. 2013). Evidence suggests that anthropogenic activities occurred throughout the shelter, affecting where and how the anthropogenic deposits have accumulated. Formation process at Diepkloof rock shelter were analysed to infer patterns of human behaviour and the geological development of the cave (Miller et al. 2013; Tribolo et al. 2013). Over 50 stratigraphic units of complex geological components were recognised through microfacies analysis and categorised into four lithostratigraphic units (LUs), then subcategorised into smaller individual microfacies units (Miller et al. 2013:3433).

LU 1 had the lowest percentage of anthropogenic material, forming largely through biogenic and geogenic process instead of human activity. This unit was dated to the post HP, late HP and halfway through the intermediate HP (Miller et al. 2013:3433). Occupation intensified during LU2 (associated to the later stage of the intermediate HP), but geogenic processes still dominated (Miller et al. 2013:3433, 3449). Behavioural traits were determined using the frequency and characteristics of combustion features. New hearths were constructed over previous hearths which were trampled, flattened, and left unused for a great period (Miller et al. 2013:3449). They were not managed or cleaned and were instead abandoned after use. LU 2 also presents with spatially variable hearth positioning, leading the researchers to believe the site was used on a relatively brief basis, yet repetitively visited (Miller et al. 2013:3449).

The shift from LU 2 to LU 3 is characterised by a sharp change in sediment which is markedly different from the underlying and overlying sequence. This unit is bracketed between 89 ka and >107 ka (Miller et al. 2013:3433). The sediment is mostly homogenous and higher in diagenetic minerals, with no clear evidence of combustion features (Miller et al. 2013:3449). However, the presence of other human occupation signals suggests the site was used frequently, such as the increase in artefacts and presence of trampled surfaces (Miller et al. 2013:3449). The authors offer another alternative for the lack of combustion features: these activities may have been conducted outside the excavation area, marking a shift in the spatial arrangement of burning activities (Miller et al. 2013:3449).

They identified a shift in hearth characteristics, ash-dumping and the burning of bedding as new behavioural activities in LU4 (>100 ka) (Miller et al. 2013:3433, 3449). The sedimentary structure comprised of distinctive MF units that accumulated from multiple and complex instances of occupation and activities (Miller et al. 2013:3450). Everyday living was different from the previous inhabitants: excessive surface trampling evolved into the preparation and use of organic bedding that was later burnt, hearth maintenance and cleaning (Miller et al. 2013:3450). Site maintenance is important for understanding the duration of occupation as it reflects repeated or longer-term site use.

Diepkloof has demonstrated the importance of the Western Cape region to the wider subject of understanding early human behaviour. The study produced a detailed insight into early the activities conducted by early modern humans, and the techniques used demonstrate the importance of using site formation as a tool to understand early human behaviour and occupation patterns.

2.2.5 Klipfonteinrand

Archaeological investigations at Klipfonteinrand have contribute further knowledge into the relationship between modern humans and climate change. The site is located 76 km from the modern coastline and was excavated in 1969 and then re-excavated between 2011-2012 (Figure 1) (Mackay et al. 2020:370). Occupation extends back to the early MSA, although the site provides valuable evidence during MIS 2 for the study of climate and human interaction (Mackay et al. 2020:363). MIS 2 experienced multiple large shifts in local climate and vegetation that is associated with a 0.7-meter sediment stack found at the back of the cave (Mackay et al. 2020:363). Such climate shifts include a rising sea level event associated with the last glacial termination, which may have unfolded rapidly towards the end of the sediment stack (Mackay et al. 2020:363). The climate record suggests that vegetation change and abrupt rises in sea level would have driven local scale changes to cultural interaction which may have had broader implications on human behaviour.

Radiocarbon dates obtained from isolated charcoal fragments revealed repetitive occupation between ~22–13 ka, with the main period of occupation occurring between 19–15 ka (Mackay et al. 2020:372, 390). Anthropogenic sediment accumulated consistently during the main occupation period, ceased for a period of 1.6 ka and then returned to similar rates after this hiatus (Mackay et al. 2020:372). Anthropogenic signals were replaced by geogenic material between 15-16 ka, suggesting lower occupation intensity (Mackay et al. 2020:372).

Located 13km away, the Doring River was utilised with greater intensity in response to declining moisture availability, increasing the frequency of retouched flakes sourced from the Doring (Mackay et al. 2020:390). The need for a permeant water source drove behavioural adaption and led to a change in material for the making of stone tools. Mackay et al. (2020) suggests a greater reliance on the Doring is consistent with patterns of decreased core distribution, and the accumulation of geogenic sediment (Mackay et al. 2020:390).

Their analysis shows a clear correlation between technological and behavioural changes in response to fluctuating environmental conditions, both in the interior and coastal regions of the Western Cape. Assemblages for both regions show clear contrasts between lithic technology, most likely reflecting instances of locally adaptive responses to environmental change (Mackay et al. 2020:391). However, an overall pattern is seen for the Robberg as the sequence for declining humidity corresponds with adaptive behaviours on both the interior and the coast (Mackay et al. 2020:391). The termination of Robberg technology for the interior also correlates with declining humidity.

Cultural interaction throughout the Cederberg may have also been driven by Meltwater Pulse 1A (14.2–13.6 ka), a dramatic event of global sea level rise (Mackay et al. 2020:391). Lithic characteristics between 15–13 ka is believed to have changed due to strengthened interaction between the populations of the coast and interior, possibly necessitated by local declining humidity and sea level rise (Mackay et al. 2020:391). Mackay et al. (2020) put forth a sequence as follows; the declining humidity which occurred during the end of the Robberg forced behavioural adaptions that differ for the interior and coastal region. Populations in the interior relied more heavily on consistent water sources such as the Doring, leading to a change in the type of materials used for stone tool production (Mackay et al. 2020:391-2). The coastal sites present with different technologies, and thus is consistent with an adaption to whatever local resources were available in the area. Growing interaction and exchange links with sea level transgression and declining humidity characteristic of the last glacial, and further increased around the major Meltwater Pulse 1A sea level event (Mackay et al. 2020:392). Klipfonteinrand highlights the extent to which climate change effected the behaviour of Cederberg populations and how this ultimately necessitated locally adaptive responses.

2.2.6 Klein Kliphuis

Klein Kliphuis is located 200 km from Cape Town, situated in a cliff above the Kliphuis River (Figure 1). The site is one of numerous in the area to contain a Late Pleistocene record after an excavation in 1984 found HP and post-HP technology (Mackay 2010; Mackay 2011). The site conforms to the general sequence of periodic occupation and was abandoned during MIS 3.

A subsequent excavation in 2006 obtained OSL (Optically Stimulated Luminescence) dates of 66 ka and 65 ka for the basal layers, marking the beginning of anthropogenic accumulation at around 65-68 ka (Mackay 2010; Mackay 2011). The rate of artefact accumulation remains steady from ~68 ka to around ~55 ka (Mackay 2010). After this date artefact density reduces dramatically, and if the dates are accepted, does not return to a similar rate until ~22 ka (Mackay 2010). This suggests a major decline in site use for a span of around 30 ka that changed the dynamic of occupation from generally consistent to episodic.

Lithics were analysed to examine the transition between the HP and post-Howiesons Poort (post HP). The site has become important to the debate discussed in section 3.2 because of the rich history of these technologies. Similar to findings at Rose Cottage Cave and Klasies River, the assemblage showed that the lithics underwent a gradual change in characteristics between the two industries (Mackay 2010; Mackay 2011). Support for this argument lies in the gradual shift in material selection (silcrete to quartzite), and the gradual increase in size and width over the transition (Mackay 2011). The results potentially rule out certain hypotheses regarding the disappearance of these industries. They identified that the data is unlikely to support periods of disrupted occupation for the end of the HP, as argued by Jacobs et al. (2008), and also explanations where population was a primary factor (Mackay 2011). They argue for a possible environmental driver because of the transition's association with MIS4/3 but express the need for new evidence to link hemispheric and local scale climate changes to associate a possible cause (Mackay 2011).

2.2.7 Putslaagte 8

PL8 is also included in the model that attests to weak occupation during MIS 3. The site is located 82 km from the present coastline, above the ephemeral Putslaagte River (Figure 1) (Mackay et al. 2015:74). The site has a late Pleistocene occupation sequence that is dated beyond 75 ka (Mackay et al. 2015:71).

Artefact density was at its peak during the LGM and occupation was largely episodic and weak between 50-22 ka. Based on OSL and AMS dating methods, the main occupation phase most likely occurred in three main stages during the LGM — c. 25-22 ka, 21-18 ka, and 18-17 ka (Mackay et al. 2015:92). High rates of anthropogenic sediment indicate occupation was at its strongest during these three stages. The introduction of marine shell and increased hornfels prevalence may imply cultural interaction between the interior and the coast that is not seen previously in the sequence (Mackay et al. 2015). A significant hiatus is seen from 25 ka until around 50 ka. Occupation is sparsely represented between 42-36 ka by low artefact density, demonstrating a substantially low percentage of occupation throughout the period of 25-50 ka (Mackay et al. 2015). One weak occupation pulse is registered for MIS 4 despite sites further into the WRZ recording highly elevated levels of artefact discard rates — e.g., Sibudu (Lombard 2008), Rose Cottage Cave (Valladas et al. 2005). Nevertheless, Boomplaas and Diepkloof share similar occupation patterns to PL8 and is thus not uncharacteristic for the immediate vicinity during MIS 4.

The MIS 4 section for PL8 were dated to 62, 66 and 65 ka and recorded a sedimentation rate of less than 100 mm/yr with as little as 300 artefacts deposited (Mackay et al. 2015:89, 93). A later occupation layer gave an age of 75.5 ± 6.0 ka (Mackay et al. 2015:90). Pre-MIS 4 deposits containing multiple layers of archaeological components were also discovered but were left undated. These occupation pulses may continue into MIS 6 but require further analysis to make an appropriate conclusion (Mackay et al. 2015:90).

2.2.8 The importance of Western Cape river systems for human occupation

The Doring River is largely responsible for sustaining the life of early humans who were concentrating their occupation around the Doring River catchment (Figure 1). Regular use of the Doring has resulted in the accumulation of large artefact assemblages on the banks of the river (e.g., Klein Hoek - Ames et al. 2020b, Putslaagte 1 - Shaw et al. 2019:404). Erosion has often distributed these assemblages across large distances, but they still contain a wealthy array of stone tools and artefacts that are important to Western Cape archaeology (here on referred to as open-air sites/localities) (Ames et al. 2020:394b).

Covering around 28,000 km2, the Doring's flow is reliant on seasonal rainfall. Consistent flow begins around May/June with the start of the austral winter rains, before reducing to a large chain of water holes in the summer (Mackay et al. 2019:370; Shaw et al. 2019:404). These waterholes persist until flow begins again in the winter, meaning a constant supply of water is still present annually (Shaw et al. 2019:404). The Doring is the only river in this region with a consistent annual flow, for example rivers in the eastern tributaries like the Bos and Tankwa Rivers which connects to the Tankwa Karoo are completely reliant on heavy rain (Shaw et al. 2019:404). Ponded water is more likely to be retained in the western tributaries, and prominent rivers such as the Groot and Biedouw sustain flow into early summer (Figure 1) (Shaw et al. 2019:404).

The human record for the Doring ranges back from the Middle Pleistocene to the Indigenous and colonial pastoralist periods (Shaw et al. 2019:404). The Middle Pleistocene date range is based on bifacial artefacts found at the nearby Uitspankraal 1 site which presents with Early Stone Age characteristics (Shaw et al. 2019:404). Surveys of the region have demonstrated an extensive array of stone artefacts on both upstream and downstream sides of the river, while lithics found at sites further from the river (e.g., Mertenhof, Putslaagte 8, Klipfonteinrand, Uitspankraal 7) suggest that it was also relied upon as a material source (Ames et al. 2020; Low et al. 2017, Low and Mackay 2018; Philips et al. 2023; Schmidt and Mackay 2016; Shaw et al. 2019:404). The area is unique in regard to flakeable lithic material and so was the main source of cobble formed-hornfels, a common material seen in lithic deposits of the Late Pleistocene (Low and Mackay 2018:171). The high rate of artefact acquisition demonstrates the intensity in which this river was utilised by early humans, not just for water but also lithic acquisition.

Local climate change is responsible for a decrease in site use that intensified occupation along the Doring. This trend is observed in multiple sites around the catchment and is just one example of how localised climate change effected the behaviour, travel, and adaption of modern humans. For example, a gradual decline in moisture availability at the site of Klipfonteinrand (located 13 km from the Doring) may have intensified the relationship between the site and the Doring River (Mackay et al. 2019). Combined with limited options for consistent water supplies, a shift in occupation towards the Doring was observed based on changes in lithic material. The river also plays a major role in the proposed 'depopulation model' of the area during MIS 3, a period of intense climate instability. Following the discovery of large lithic assemblages at the open-air site of Putslaagte 1, a new theory suggests rock shelters were abandoned in favour of permeant water sources (Mackay et al. 2014). Occupation became centred around the Doring River which led to a decline in rock shelter use.

2.3 Broad environmental history of South Africa

South Africa has experienced major climate fluctuations from at least the past 130,000 years (Table 2). The Last Interglacial (130,000-118,000 ka) and Last Glacial period (roughly 64,000-32,000 ka; Deacon and Deacon 1999) was marked by a number of interglacial/glacial events that are associated with various MIS (Marine Isotope Stage) periods, MIS 5d-5a (105-82 ka) MIS 4 (75-59 ka), MIS 3 (64-32 ka) and MIS 2 (29-12 ka) (Deacon and Deacon 1999:22; Henshilwood 2008). The early Last Glacial experienced minor climate fluctuations, characterising MIS 4 with cold conditions almost relative to the LGM (Last Glacial Maximum) (Deacon and Deacon 1999:22)

A cool climate persisted throughout the LGM (24,000-18,000 ka), caused by the formation of large continental ice sheets in the northern high latitudes (Deacon and Deacon 1999:21). Conditions were generally cold, dry and windy until 16,000 ka, where climate improves. Frost heaving occurred instead of glaciers, while the Cape mountains witnessed near-glacial conditions (Boelhouwers 1999; Deacon and Deacon 1999:21). From 16,000 ka during the Late Glacial (18,000-11,500 BP; Chase and Meadows 2007:106) higher precipitation is suggested based on the acquisition of more permanent water in the Northern Cape (Deacon and Deacon 1999:21).

Around 12,000 ka marks a switch from the cooler climate of the Late Glacial and LGM to the warmer conditions of the present Interglacial, representing MIS 1 (12,000 ka to present) (Deacon and Deacon 1999:21-22). This period is referred to as the Holocene and was marked by highly variable climate changes (Chase and Meadows 2007; Deacon and Deacon 1999:21; Mayewski et al. 2018). The Holocene Altithermal (HA) (8,000-4,500) was the warmest period for the Holocene with conditions reaching 2-3°C above present day temperatures, reaching its peak between 7,000-4,500 BP based on evidence from Wonderkrater and Boomplaas Cave (Chase and Meadows

2007:112). A 0.5°C and 3°C drop in temperature is seen at Uitenhage between 4,000-2,000 BP, broadly relating to similar findings in the southwestern Cape at Tortoise Cave, and South America and Australia (Chase and Meadows 2007:112).

Today, South Africa’s environment is highly influenced by a wide range of oceanic, seasonal and atmospheric systems. The annual average of rainfall varies significantly in accordance with season and droughts are frequent throughout the region (Monteath 2001:4).

Climate Stages (ka)	Climate Conditions in South Africa
Last Interglacial: 130,000-118,000	- Multiple interglacial events occurring at 103,000 ka, 84,000 ka 60,000 ka and 32,000 ka
Last Glacial: 64,000-32,000	- Early Last Glacial marked by cold conditions similar to LGM climate
LGM: 24,000-18,000	- Cold, dry and windy with frost heaving of the ground
Late Glacial: 18,000-11,500	- Higher precipitation
Present Interglacial: 12,000-Present	- Increasingly warm climate and highly variable - 2-3°C above present day temperatures between 7,000-4,500 - 0.5 °C and 3 °C temperature drop between 4,000-2,000

Table 2 Overview of South African climate change over the past 130,000 years to present.

2.4 Contemporary vegetation and environment, Western Cape

Before an accurate paleoenvironmental reconstruction can be achieved on any area of the southwestern Cape province, the complexity of the regions modern environment must be considered. As suggested by Meadows and Baxter (1999), any paleo-reconstructions of the region will most likely be spatially variable. Therefore, because the contemporary region has different environments there is a reason to assume that the environments of the Quaternary (the last 2.6

Ma) (Valsecchi et al. 2013) would be neither directional nor consistent throughout the region (Meadows and Baxter 1999:194).

The southwestern Cape landscape is unique in its cultural, geological, environmental, and topographical characteristics. It is known for its distinctive vegetation of *fynbos* type plant species (a fine-leaved, fire adapted Sclerophyllous shrub; see section 2.5.2) which is prevalent throughout much of southwestern South Africa (Meadows and Baxter 1999:194-5; Meadows and Sugden 1991a; Wells 1991:118).

The complexity of the WRZ's environmental conditions is apparent from studies of pollen (Chase and Meadows 2007; Parkington et al. 2000), charcoal (Cowling et al. 1999; Mackay and Cartwright 2022; Mitchell 2008) and isotopic change in marine sediment (Chase and Thomas 2007; Henshilwood 2008) which allow a reliable documentation of climate change. When coupled with archaeological investigations a general pattern of occupation and human behaviour can be inferred.

2.4.1 MIS 5b to MIS 3

During the MIS 5b (95-85 ka) and MIS 5a (90-70 ka), climate conditions in the Cape province were cool with strong westerly winds that intensified aeolian deposition notably around 90-88 ka (Henshilwood 2008:41). Sea levels were 40-60 m lower than present day and faunal data collected from sites in the southwestern Cape suggests MIS 5b was dominated by an open grassland environment with a cool and moist climate (Henshilwood 2008:41).

Climate conditions on the Southwestern Cape were most likely dry and cool between ~80–74 ka with higher moisture during the boundary between MIS 5a/4 (Henshilwood 2008:42). Significant aeolian deposition in the southern Cape during the MIS 5/4 boundary and early MIS 4 (75–59 ka) suggests the transition between these stages corresponded with colder and wetter conditions (Henshilwood 2008:42). HP (66–58 ka) technocomplex corresponds to later MIS 4 and continues into MIS 3.

The start of MIS 4 in the Cape region was met by a major decline in sea level at ~70 ka and a colder and drier climate (Henshilwood 2008:43). Between MIS 5a/4 sea levels declined globally over a period of 6 ka at a rate of 10 m every thousand years (Henshilwood 2008:43). Along the coast during the HP, Diepkloof experienced a decline in humidity (Mackay and Cartwright 2022:7). Additional data from aeolian deposits along the west coast show a distinctive peak in regional scale aeolian activity at 73–63 ka (Chase and Thomas 2007:35).

An in-depth temperature index created by Thackeray (2002) at the Die Kelders 1 site indicates a decline in temperature from 15.2 to 13.4°C that corresponds to MIS 4 (75–59 ka) (Thackeray 2002:750). The coldest period of MIS 4 (ca. 55 ka) retained a temperature of 13.8°C (Thackeray

2002:751). Significant roof fall and limited anthropogenic material may be associated with this relatively low temperature, although shifts in moisture are suggested as the primary cause of the roof fall instead of cold conditions (Thackeray 2002:751).

Towards the coast, Diepkloof experienced periods of cooler climate fluctuations characterised by wet conditions and frost shattering of the shelters during the MSA (Chase and Thomas 2007:114). Further evidence suggests a generally wetter MIS 4 followed by a humid phase between ~65–50 ka (MIS 3: 64–32 ka) (Chase and Thomas 2007:36, 114).

Elands Bay show similar cool and wet conditions based on charcoal records dating to 40,000 cal. BP (Chase and Meadows 2007:114; Chase and Thomas 2007:114). Intensification of aeolian deposition also occurred between 49–41 and 33–30 ka (Chase and Thomas 2007:35). The charcoal record from Elands Bay indicates a cool and wet climate during 40–20 ka that could support a diverse moisture-dependant Afromontane Forest and woodland vegetation (Cowling et al. 1999; Mitchell 2008:54).

Further inland towards the local area of Mertenhof, charcoal evidence from Klein Kliphuis supports declining humidity and soil moisture during the MIS 4/3 transition (Mackay and Cartwright 2022:7).

For MIS 3 Die Kelders retained a temperature range between 13.1 and 14°C which roughly parallels with the temperature range interpreted for the Klasies River Mouth in the Southern Cape coast (Thackeray 2002:751). Around 31 ka temperature was still around 13°C and then drops to a low of 11.7°C towards the very end of MIS 3 (Thackeray 2002:751). This layer is associated with collapsed roof fall and is similar to the coldest conditions of the LGM. The overlaying layers retain warmer temperatures of 15.9°C and 14.4°C (Thackeray 2002:751).

Overall, the Western Cape experienced severe oscillations of cold and moist conditions with phases of intense aeolian activity over the period of 95–59 ka. Around the MIS 5/4 transition conditions deteriorated in the form of lowered sea level and a climate shift from dry and cool to cold and wet conditions. The utilisation of rock shelters during early MIS 4 in the southwestern region (for example Die Kelders, Elands Bay) may have been caused by an increasingly severe climatic period (Butzer 2004:1778; Henshilwood 2008:10).

Age	Environmental Conditions	Temperature Index from Die Kelders 1	
MIS 5b/a 95-70 ka	Cool and windy with a 40-60 m low sea level and an open grassland landscape.		
90-88 ka	Intense aeolian deposition		
80-74 ka	Dry and cool, moisture increase around MIS 5a/4 transition.		
70 ka	Colder and dryer marked by major decline in sea level.	MIS 4	Decline from 15.2 to 13.4 °C
65,000–50,000 ka	Declining humidity and soil moisture between MIS 4/3 transition (Klein Kliphuis).	55 ka	13.8 °C
MIS 3		MIS 3	Between 13.1 and 14 °C
49-41 ka	Phase of aeolian deposition		
40-20 ka	Cool and wet climate at Elands Bay		
33-30 ka	Phase of aeolian deposition	31,800 ka	Drop from 13°C to 11.7°C

Table 3 Climate conditions in the Western Cape between MIS 5b to 30 ka, coupled with the temperature index from Die Kelders 1 (Chase and Thomas 2007; Cowling et al. 1999; Henshilwood 2008; Mackay and Cartwright 2022; Mitchell 2008:54; Thackeray 2002).

2.4.2 MIS 2

MIS 2 is characterised by a cool and moist climate for the Western Cape and a cool and dry climate for the Southern Cape. The Western Cape Mountain region (Figure 2) experienced an 8–10°C cooler climate for the winter months during the LGM, based on periglacial features like gelifluction sheets and ice-wedge casts (Boelhouwers 1999; Boelhouwers and Meiklejohn 2002; Chase and Meadows 2007:110-111; Meadows and Baxter 1999:205). Rising 2249 m asl (above sea level), Matroosberg is situated in the Hex River and is the highest summit in the Western Cape Mountain region (Boelhouwers 1999:246). Boelhouwers' (1999) study of frost weathering on the periglacial block streams and terraces of Matroosberg suggests this resulted in high amounts of blocky debris followed by frost creep, resulting in an annual temperature of around 0°C

(Boelhouwers 1999:256; Boelhouwers and Meiklejohn 2002:51). Modern day temperatures in this region are now around 7–8°C (Boelhouwers 1999:256; Boelhouwers and Meiklejohn 2002:51).

Meadows and Baxter (1999) also associate this region with cooler than present temperatures and a greater level of moisture availability (Meadows and Baxter 1999:205). The Southern Cape experienced a cool and dry LGM, in comparison to the Western Cape's cool and moist climate (Meadows and Baxter 1999:205). Regional scale aeolian activity occurred between 24–16 ka (Chase and Thomas 2007:35).

Sedimentary layers containing pollen at Elands Bay point to a significant extension of the winter rainfall season during the LGM, supporting the findings of Meadows and Baxter (1999) and Scott and Woodborne (2007b) (Chase and Meadows 2007:116; Chase and Thomas 2007:35; Parkington et al. 2000).

2.4.3 MIS 1

MIS 1 climate conditions are generally characterised by a warming trend with oscillations between drier and more humid phases. Coupled with other late Holocene climate reconstructions from the western coast region (Benito et al. 2011; Stager et al. 2012), Weldeab et al. (2013) agree that the WRZ was highly influenced by centennial and millennial-degree climate change. Their findings contribute to the possible link between westerly winds from the Southern Hemisphere and Agulhas water leakage, causing large fluctuations in WRZ climate (Weldeab et al. 2013:2348).

Weldeab et al. (2013) identified millennial scale environmental fluctuations consisting of three periods during the early and middle Holocene. Grain size analysis conducted on samples from the Orange River show a high percentage of fine sediments which indicates the Orange River played a dominate role for increases in fluvial input in the early Holocene (Weldeab et al. 2013:2356). Slight shifts in $^{143}Nd/^{144}Nd$ ratios (εNd) towards the coast and the level of fine sediment left behind has been interpreted to suggest a wet climate between 11 and 9500 cal years BP for the coastal region (Weldeab et al. 2013:2356). A trend of declining sediment and εNd values around 9200 cal years BP, and a corresponding increase of grain size which reaches its peak around 6000 and 5500 cal years BP indicates a reduced sediment value for the Orange River, in comparison to higher percentages of coarse grains for the coastal region (Weldeab et al. 2013:2356).

A relatively consistent pattern for climate variability on a regional scale is seen for the WRZ (Table 2). Carbon and nitrogen isotopes and pollen time series data from the western WRZ (Scott and Woodborne 2007a, b) indicate enhanced moisture content with a warming climate from 12000 and 9500 cal years BP (Scott and Woodborne 2007a:947; Weldeab et al. 2013:2357). Aridity replaces this environment around 8500 cal years BP, persisting until 5600 cal years BP (Scott and Woodborne 2007a:948).

The date for the onset of arid conditions correlate with Weldeab et al. (2013) findings of increases in coarse terrigenous sediment, which they have interpreted as dust mobilisation due to an arid climate (Scott and Woodborne 2007a:947; Weldeab et al. 2013:2357). In the coastal region the wet periods correlate with cold surface water and strong upwelling. Ongoing aridification in the mid-Holocene correspond with a deterioration in the southern Benguela Upwelling System which is also consistent with latitudinal shifts in austral westerlies and fluctuating Agulhas water leakage (Weldeab et al. 2013:2361).

The middle Holocene in the WRZ saw a continuous period of aridification that reached its peak around 5500 cal years BP (Weldeab et al. 2013:2360). Weakening of the upwelling system and a rise in dust deposits correspond with a decrease in SE trade wind, and supplementary leakage of Agulhas water (Weldeab et al. 2013:2360).

These systems subjected the WRZ to two different climates: an increasingly wetter climate for the coastal region for the last 600 cal years BP, and amplified precipitation for the west (Chase and Meadows 2007:108; Weldeab et al. 2013:2360). This supports Meadows and Baxter's (1999) hypothesis that glacial climate was variable throughout the WRZ (Chase and Meadows 2007:108). Consequently, elements of the south coast paleoenvironment cannot be generalised for the whole WRZ as subregions experienced drastically different climates.

As for the immediate WRZ of the southwestern Cape Meadows and Baxter (1999) split the period up into two distinctive halves, the first half associated with warm and dry conditions. The second holds similarities to contemporary temperatures but with more freely available moisture (Meadows and Baxter 1999:204).

A pollen core covering the past 17,600 cal yr BP from Driehoek Vlei in the central Cederberg Mountain range identified a continues decline in Clanwilliam cedar, demonstrating a climate transition between wet glacial conditions to a warm and dry Holocene (Meadows and Sugden 1990; Meadows and Sugden 1991a; Meadows and Sugden 1991b; Meadows and Sugden 1993). Post glacial warming is supported at Pakhuis Pass Shelter around 16 ka (Scott and Woodborne 2007b:131). Boomplaas and Wonderkrater also supports a time of rapid warming that can be confirmed by changes in the temperate curve of the Vostok ice core in Antarctica around 17 ka (Chase and Meadows 2007:111). At Elands Bay, greater moisture availability is noted particularly between 13-11.3 ka (Parkington et al. 2000:544).

The pollen record at De Rif midden in the Cederberg showed a highly unstable climatic since at least the LGIT. The sites experienced variation in fire frequency and high levels of vegetation fluctuation (Valsecchi et al. 2013.

Estimated Age Range:	Coastal Region:	Western Region:
LGM	Extension of winter rainfall season on the west coast based on non-drought tolerant plant species.	
12-9.5 BP		Increased moisture content and warming climate based on carbon and nitrogen isotopes and pollen data.
13-11.3 ka	Greater moisture availability on west coast.	
11-9.5 BP	Shifts in 143Nd / 144Nd ratios show a wetter climate.	
8500-5600 BP		Pollen records point to an arid climate.
Last 600 years BP	Wetter climate.	Increased precipitation.

Table 4 Climate record spanning from the LGM showing the variable climate within the Coastal and Western sections of the WRZ.

2.5 Mertenhof rock shelter

2.5.1 Site setting

Located c. 250 km north of Cape Town in the Western Cape of South Africa, Mertenhof rock shelter is situated in a low-lying ravine above the Biedouw River catchment on the eastern flanks of the Cederberg Mountains (Figure 2, Figure 3) (Low and Mackay 2018:171, 174; Schmidt and Mackay 2016:3). The site is elevated at a height of ~25 meters above the Biedouw River and ~600 m.a.s.l (meters above sea level), and is carved into a quartzite cliff face (Figure 3) (Williams 2017:33, 34). From the dripline Mertenhof measures ~9 m deep and reaches up to 4.2 m heigh (Williams 2017:35). It covers a floor area of ~70 m^2 and the entrance to the shelter measures a width of ~10 m (Figure 4) (Williams 2017:35).

Figure removed due to copyright restriction

Figure 2 Map showing the location of Mertenhof rock shelter within the Western Cape region. Based on data from Williams 2017.

Figure 3 Inside of Mertenhof rock shelter after the 2017 excavation. (Photograph: Ian Moffat).

2.5.2 Climate, vegetation and hydrology

The area is semi-arid with a typical rainfall of <250 mm annually, with >66% falling between April to September (Ames et al. 2020:2a; Chase and Meadows 2007:104; Weldeab et al. 2013:2348). Vegetation consists of low shrubbery of Fynbos and Succulent Karoo types, although is relatively sparse (Ames et al. 2020:2a; Schmidt and Mackay 2016:3; Wells 1991:115). The Fynbos biome is restricted to the Cape Fold Belt mountains and the coast, occurring in both the winter and all-year rainfall zones. (Mitchell 2002:23). Sclerophyllous shrub and heathland are dominant, and fire-adapted plants that require fire to re-germinate are common throughout the area (Mitchell 2002:23; Wells 1991:118).

While the catchment is moderately small, the Biedouw River provides a steady supply of year-round running water, although is greatly reduced by the warmer weather (Schmidt and Mackay 2016:3-4). The reliance on a consistent water supply is hypothesised for the sites relatively steady occupational history, unlike other sites which rely on the Doring River (Low and Mackay 2018:174; Schmidt and Mackay 2016:4). The site is approximately 19 km northeast of the Doring, and has been a centre for human occupation since at least the Middle Pleistocene (Ames et al. 2020:2a; Low and Mackay 2018:174; Schmidt and Mackay 2016:3; Shaw et al. 2019:404).

2.5.3 Archaeological excavations at Mertenhof

Archaeological investigations at Mertenhof were undertaken between 2013-2017 where a 3 m x 2 m trench was excavated over the course of 5 seasons. The trench was split into six-one-meter squares (SQ1, SQ2, SQ3, SQ4, SQ5, SQ6) (Figure 3). A child burial was encountered which required the opening of a partial seventh square to allow for recovery. Archaeological material (e.g., stone artefacts, bones, ostrich eggshell, ochre) smaller than <15 mm were piece plotted and beads, worked bone and stone lithics such as bladelets, cores and retouched flakes were plotted with a total station regardless of size. Other material (e.g., sediment) were sieved on site through 3 mm and 1 mm sieves. On the completion of excavation an estimated 22,000 objects were plotted overall. A maximum excavation depth of 1.9 m was reached in SQ4 and bedrock is yet to be reached. Bioturbation from moles and termites has affected the stratigraphic integrity significantly, causing reworking of the upper late Holocene and terminal Pleistocene deposits. No finely laminated stratigraphic features were present, but 10-30 cm scale units were identified. GPR (ground penetrating radar) and ERT (electrical resistance tomography) were conducted on the surface of the cave as part of the 2017 excavation.

Figure 4 Photo depicting the positions of each excavation square. Depth unknown. (Photograph: Ian Moffat).

2.5.4 Previous archaeological study at Mertenhof

Previous archaeological study of the site has revealed a distinctive pattern of heat treated lithics that are not consistent with other sites in the Western Cape. This evidence has questioned the theory surrounding why and how heat treatment was used, generating a new hypothesis on the use of heat treatment in the area.

The application of heat treatment to stone artefacts was a fire-based techniques used by early humans to modify the mechanical properties of raw lithic material (Schmidt and Mackay 2016:2; Schmidt et al. 2020:1; Stolarczyk and Schmidt 2018:1). Once heat treated, the fracture properties of silcrete becomes similar to finer grained material such as chert and allows for an easier and more refined knapping outcome (Schmidt and Mackay 2016:2; Sealy 2009:323). Many aspects of this technology are still under debate, with questions surrounding when it was first established in the Cape region, and what it means for early *Homo sapien* behaviour (Schmidt and Mackay 2016:2; Schmidt et al. 2020:1). The ability to apply this technique for the first time is commonly associated with an experienced understanding of fire, a high level of cognitive ability, and a wide range of problem-solving and goal-oriented behaviours (Sealy 2009:323; Stolarczyk and Schmidt 2018:8).

Heat treatment was implemented around 130 ka in the Cape coastal zone (Schmidt et al. 2020:8). The HP and SB were the main periods for heat treatment: the majority of silcrete was treated at Pinnacle Point between 71 and 60 ka (Brown et al. 2009), was applied to 92% of HP silcrete at Klipdrift Shelter (Schmidt et al. 2016), and to the majority of silcrete at Hollow rock shelter (Schmidt and Högberg 2018). However, Mertenhof is the exception as it presents with inconsistent patterns of heat treatment (Schmidt and Mackay 2016:13; Schmidt et al. 2020:8-9).

The argument that heat treatment was a necessary application for the manufacture of stone artefacts is not consistent with the evidence found at Mertenhof. Schmidt and Mackay (2016) found a link between the frequency of heat treatment and fine-grained material such as chert. Their argument stems from the fact that if heat treatment transforms silcrete's mechanical properties into one similar to chert, then an abundance of chert would limit the need for heat treatment. Their findings are consistent with this interpretation as a clear pattern between chert and heat treatment were found (Schmidt and Mackay 2016:9). The HP presents with a regular occurrence of flaked and discarded silcrete which was not heat treated (Schmidt and Mackay 2016:13). Therefore heat treatment of silcrete was not required to successfully transform the material into workable tools, nor does an increase in silcrete prevalence suggest heat treatment was used more frequently (Schmidt and Mackay 2016:13; Schmidt et al. 2020:8-9). Because Mertenhof shows silcrete can, and was, used without heat treatment, the site challenges the theory that this technique was a necessary application for stone tool knapping (Schmidt and Mackay 2016:13; Schmidt et al. 2020:8-9).

2.5.5 Variation in Robberg Blade Technology from Putslaagte 8, Klipfonteinrand and Mertenhof

The production of small unretouched blades can be defined as the earliest examples of stone artefact manufacture for the Later Stone Age (LSA) (Low and Mackay 2018:168; Lombard et al. 2012). These blades, otherwise known as Robberg Blade technology, are largely dominant throughout South African lithic assemblages between 22-12 ka (Low and Mackay 2018:168). Robberg assemblages from three sites along the Doring, Putslaagte 8 (PL8), Klipfonteinrand and Mertenhof, were analysed to identify if the availability of local raw material influenced the production of blade technology. The sites are located roughly 10-15 kms apart and contain rich assemblages of Robberg technology dating between 18-22 ka (Low and Mackay 2018:171).

Low and Mackay (2018)'s analysis showed interesting patterns of blade material in response to distance from the Doring. Lithic characteristics and material at PL8, Klipfonteinrand and Mertenhof vary across each site (Low and Mackay 2018:179). Locally sourced quartz, fine-grained siliceous and crypto-crystalline silicate lithologies increase in relation to distance from the Doring, while silcrete decreases. Although quartz increases with distance, this increase does not apply for the frequency in which bipolar techniques were used: nearly 80% of PL8 quartz lithics were knapped using bipolar methods, decreasing to nearly a third in the other two site's quartz assemblages (Low and Mackay 2018:179). This implies quartz was treated differently according to site location (Low and Mackay 2018:181). Quartz lithics were smaller at Klipfonteinrand and Mertenhof and larger at PL8 (Low and Mackay 2018:183).

The decrease in hornfels and silcrete, and the increased in quartz with distance from the Doring has been attributed to the opportunistic local procurement of lithic sources in the area. Therefore, it seems Robberg technology was produced from situational raw material, and methods and techniques were not uniform across all sites.

2.5.6 Occupation sequence for Mertenhof

Mertenhof was the subject of another postgraduate thesis that employed a similar range of geoarchaeological techniques to study chronology and site formation (Williams 2017). OSL dating and stratigraphic evidence was successful in determining an occupation sequence that shows occupation within or towards the end of MIS 3 (Mackay 2016; Williams 2017). As discussed in section 4.3, occupation markers during this period are rare throughout the region, reiterating the sites uniqueness and its importance to understanding local occupation patterns and behavioural adaption.

Mertenhof's site formation was largely formed by anthropogenic and aeolian (deposition by wind, Reitz and Shackley 2012:126) deposited sediment, resulting in a shallow sedimentary profile of

(~1.5-2 m) (Williams 2017:88). Sediment analysis was conducted by Williams (2017) using the x-ray diffraction method and a master-sizer for grain size analysis. Given the area is quartz-rich, it is not surprising that the x-ray diffraction results exhibited a high quartz content that ranged between 91.3% and 84.6% (Williams 2017:41). Grain size showed a clear pattern of coarseness towards the front of the cave, becoming finer towards the rear (Williams 2017:41). The structure of the cave (the profile narrows towards the rear of the cave) probably prevented human activity towards the back, and so the difference in grain size is consistent with cave use that was largely centred towards the front of the cave (Williams 2017:88). Around 34 ka the stratigraphy slopes significantly towards the back of the rock shelter caused by limited anthropogenic input and sediment build-up (Williams 2017:88).

Anthropogenic material permitted the reconstruction of occupation. Associated OSL dating prove Mertenhof was in fact occupied during MIS 3. The stratigraphic sequence is as follows: The top layer (*StratAgg* ULBD) was dated to around <2 ka (Williams 2017:40) (Table 5). Pottery and stone artefacts suggest an age younger than 2,100 ka, and glass beads place occupation within the last 500 years (Williams 2017:40). 572 artefacts were recovered (Will et al. 2015:13). A possible hiatus is seen between ULBD and R/GBS. R/GBS retained a date of 16-22 ka and was dominated by Robberg industry technology and 1043 total artefacts (Williams 2017:40; Will et al. 2015:13). VDGS produced the same age range (16-22 ka) and was also highly dominated by Robberg-type lithics. A hiatus in occupation between 22-25 ka is inferred by Mackay (2016). *StratLayer* CWGS, and *StratAgg's* LGS, LRS and DGS date to various stages throughout MIS 3. OSL results for *StratLayer* CWGS generated an age of 34.1 ± 1.4 ka and had a sedimentological make up that changed from sandy to silty with depth and thickened towards the rear of the shelter (Williams 2017:40). The LGS layer contained evidence of human occupation in the form of blade technology and decaying hornfels, retaining a date of 40.8 ± 1.8 ka (Williams 2017:40). 782 total artefacts were recovered (Will et al. 2015:13). Dated to 49.4 ± 2.0 ka, LRS recorded 702 total artefacts (Will et al. 2015:13), a change in lithic technology that is characteristic of the MSA, disc-shaped flakes and cores, and higher percentages of decayed white stone (Williams 2017:40). DGS held an abundance of late post-HP technology and 876 total artefacts (Will et al. 2015:13), dating to 50-55 ka (Williams 2017:40).

Further chronology is supplied by Mackay (2016). Preceding DGS are two rich occupation layers (upper BGG/WS – 3227 total artefacts and lower BGG/WS – 2561 total artefacts) (Will et al. 2015:13) containing post-HP and HP archaeology. RGS contained a limited number of bifacial points characteristics of the SB period (444 total artefacts) (Will et al. 2015:13). A further sedimentary unit (DBS) was classed as early MSA but requires further study to be definitive (Mackay 2016:6). 339 total artefacts were recovered (Will et al. 2015:13).

Stratigraphic layer	Age	Total number of artefacts
ULBD	<2 ka	572
	Hiatus	
R/GBS	~16-22 ka	1043
	Hiatus between ~22-25 ka	
CWGS	~34 ka	
LGS	~40 ka	782
LRS	~49 ka	702
DGS	~50-55 ka	876
Upper BGG/WS	Post-HP (~58-45 ka) and HP (66-58 ka)	3227
Lower BGG/WS	Post-HP (~58-45 ka) and HP (66-58 ka)	2561
RGS	SB (~77-70 ka)	444
DBS	Early MSA	339

Table 5 Total number of artefacts with associated OSL ages.

2.6 Limitations to the study of rock shelters: MIS 3 in South Africa

While there are many advantages to the study of site formation processes in rock shelters, limitations and weaknesses have also been encountered. Because sediment accumulation is highly influenced by erosion and weathering this can affect the interpretability of site formation results. The high erosive environments of the Western Cape, and South Africa broadly, can cause issues determining signs of occupation, and the interpretation of occupational models for South Africa have been affected because of it. Another issue that is particularly relevant for the Western Cape is a strong preference for archaeological research on rock shelters over open-air localities (Mackay 2016; Mackay et al. 2014; Mitchell 2008). The nature of hunter-gatherer societies show a heavy reliance on large scale land use to conduct a multitude of everyday activities (Mackay 2016; Mackay et al. 2014:44; Mitchell 2008:61). Adaptions to changing ecologies would also necessitate relocation to different sites that may not have necessarily been rock shelters. Considering rock shelters were not always used consistently they may offer only a portion of the information needed to infer past behaviour.

These issues are particularly prevalent in the depopulation model of southern Africa during MIS 3 which only came to light after further research was performed on further rock shelter sites in the Western Cape. Based on a small pool of rock shelter data (e.g., Boomplaas cave, (Deacon, 1995) the WRZ once presented “little or no” occupational data that proved occupation during MIS 3 (Mackay 2010:145), despite strong evidence for population before and after the period of 50-25 ka (Mackay et al. 2014:43). This hiatus was interpreted as either the abandonment/depopulation of the region (Ambrose 2002; Klein et al. 2004) or as suggested by Deacon (1995) a bottleneck in population that resulted in little to no accumulation of archaeological deposits. Mackay et al. (2014) associates these interpretations with a lack of new research and a dominance for rock shelter archaeology that may have contributed to “misleading depictions of regional occupation” (Mackay et al. 2014:43). Based on new evidence at the open-air locality of Putslaagte 1, Mackay et al. (2014) proposes that an absence of occupational signals in rock shelters may instead be more characteristic of landscape reorganisation coupled with a more intense focus on well-watered areas along major rivers.

The site which is located ~100 m east of the Doring River, has been interpreted as a functioning flaking location that was used throughout MIS 3 (Mackay et al. 2014:53). Two OSL ages were obtained that successfully dated the artefacts to either the late MIS 4 or early MIS 3 (Mackay et al. 2014:49). Based on these dates and the depth of the analysed sediments it was inferred that the surface artefacts were most likely the result of site use during or after the period of MIS 3. Therefore, this evidence does not support the abandonment theory, but instead highlights the over-reliance of rock shelter archaeology in the Cape region. Further work on open air localities will probably show a behavioural change that resulted in a different type of occupation, instead of overall abandonment.

The abandonment of these rock shelters may be due to the reorganisation of land-use that focused on well-watered regions along the bank of the Doring River. Mackay et al. (2014) also suggests further research at sites such as Mertenhof may be useful for further exploration of land use patterns. The semi-permanent river adjacent to Mertenhof is theorised to have encouraged occupation at Mertenhof during this time. This study hopes to supply additional evidence for occupation during this period.

CHAPTER THREE: METHODS

3.1 Introduction

Sediment samples were collected from squares 4 and 6 in 2 cm increments. The laboratory methods conducted in this analysis were applied to these samples. Five geoarchaeological techniques were used to recreate Mertenhof's sedimentary history – LOI, particle size and shape, MS and ICP-elemental analysis. Thirteen OSL dates were also generated before this analysis.

3.2 Preliminary Optically Stimulated Luminescence Dating

OSL analysis has become a reliable technique in the dating of archaeological material. Major advances over the years have allowed the dating of Quaternary occupation sequencies, artefacts and sediment within a date range of >150,000 years, with an accuracy rate of as little as 5 to 10% (Bluszcz 2004; Jacobs and Roberts 2007). This technique surpasses the radiocarbon method in its ability to date beyond the limited range of 40,000 to 60,000 ka (Dincauze 2000:109; Taylor and Bar-Yosef 2014:19), and when organic material is otherwise lacking (Bluszcz 2004; Jacobs and Roberts 2007). OSL dates are produced by measuring the amount of energy an individual grain has absorbed during its last exposure to light (Jacobs and Roberts 2007:211; Murray and Wintle 2000:57).

A previous study produced 11 OSL dates for SQ4 and 5 for SQ6 at Mertenhof. These dates were obtained using two different approaches: the SAR (single-aliquot regenerative-dose) and SGC LnTn (standardised growth curve) methods. Two different dates were generated using these approaches as detailed in Table 4 and 5. The dates generated by the later method were used in this analysis. A possible outlier is evident in sample MRS13-10 (49.4 ± 2.0 ka). Bioturbation is a documented occurrence at the site and is a possible cause, but considering the discrepancy is very small an error may not have occurred.

Sample (SQ4)	**Depth**	**Associated lithic material**	**SAR (ka)**	**SGC LnTn (ka)**
MRS13-7	0.38	Late MSA	41.3 ± 1.7	41.5 ± 1.6
MRS13-8	0.50	Late MSA	50.3 ± 2.1	52.0 ± 2.6
MRS13-9	0.60	Late post-HP	53.3 ± 2.3	53.5 ± 2.2
MRS13-10	0.70	Late post-HP?	46.7 ± 1.9	49.4 ± 2.0

MRS13-11	0.75	Post HP	50.8 ± 2.4	52.4 ± 2.4
MRS13-12	0.85	Late HP	49.4 ± 2.4	54.1 ± 2.6
MRS13-13	0.95	Early HP	71.6 ± 4.6	73.6 ± 4.0
MRS13-14	1.08	Pre HP/SB	64.0 ± 2.9	74.3 ± 3.4
MRS17-4	1.37	eMSA	>125	>150
MRS17-6	1.46	eMSA	>95	>100
MRS17-7	1.63	eMSA	>90	>100

Table 6 OSL ages for the SAR and SGC LnTn methods for SQ4.

Sample (SQ6)	Depth	Associated lithic material	SAR (ka)	SGC LnTn (ka)
MRS17-8	0.40	_	21.5 ± 0.9	21.8 ± 1.2
MRS13-6	0.54	late MSA	26.6 ± 1.2	24.5 ± 1.4
MRS13-5	0.65	late MSA	35.4 ± 1.4	35.9 ± 1.4
MRS17-1	0.76	late MSA	36.1 ± 1.7	39.8 ± 2.2
MRS17-3	1.49	SB/eMSA?	>80	>100

Table 7 OSL ages for the SAR and SGC LnTn methods for SQ6.

3.3 Laboratory Methods

3.3.1 ICP elemental analysis

ICP is a geochemical method that is used to measure the concentration of elements in archaeological soils. Soil chemistry and archaeology are linked through certain anthropogenic activities which can either deplete or enhance the chemical properties of the soil. In rock shelters, long-term pollution from human induced combustion may enhance certain heavy metals in the soil, leading to high contamination or ‘paeleopollution’ (Monge et al. 2015; Oonk et al. 2009). A major problem with interpreting anthropogenic signals through heavy metals is that uncertainties still exist over which type and percentage of elements should be considered as indications of archaeology, and what these certain elements reveal about past activities (Oonk et al. 2009). Hence, it is currently difficult to associate a specific chemical signature with anthropogenic induced combustion activities, but evidence does suggest that leeching of heavy metals do occur from long-term burning. For instance, Monge et al. (2015) studied high levels of heavy metals in two archaeological caves in Gibraltar, Gorham's and Vanguard Caves. In both caves Zn (zinc) and Cu (copper) levels were found at the highest concentrations in well-preserved hearths and along the entire soil level before and after these hearths (Monge et al. 2015:5). Fire related mechanisms such as the distribution of Zn and Cu rich ash by convection may explain the high contamination of entire soil levels throughout the soil strata (Monge et al. 2015:5). Zn concentrations were also higher in observed anthropogenic layers.

Although uncertainties do lie when associating heavy metals with archaeological activities, the literature does suggest that elements such as Ca (calcium), Cu (copper), Mg (magnesium), K (potassium), Na (sodium), P (phosphorus) and Zn (zinc) do commonly occur within archaeological soils (Oonk et al. 2009:38).

Trace element analysis for sediment samples at Mertenhof were measured in a HEPA filtered clean laboratory at the University of Adelaide using the Aqua Regia digestion method. In the excavation samples were taken from the excavation face of SQ4 and SQ6 every 2 cm to allow for further analysis in the laboratory. For this method samples were analysed at 10 cm increments (samples 0-160 cm for SQ4 and samples 0-140 cm for SQ6). For each sample ~0.1 g of sediment was weighed on a precision scale accurate to 0.001 g and added to ~1 ml of deionized water. Initial cleaning of the Teflon vials involved filling the vials with 6M HCl (Hydrochloric acid) and heated to 140°C overnight on a hot plate with the caps on. They were then rinsed with deionized water and left uncapped for 48 hours in a wash carboy filled with 6M HNO3 (Nitric acid). They were again rinsed by deionized water and dried. The sediment was dissolved in a solution of 200 ml of ~12M HCL and 100 ml of ~15M NNO3, otherwise known as Aqua Regia solution, and left for 16 hours at room temperature. They were left capped at 140°C on the hotplate for 2 hours and then evaporated to dryness at 100°C with the lids removed. 5 ml of 6M HCI was added to the sample and heated to 100°C on the hotplate and then centrifuged for 10 minutes at 1300 RPM. Subsamples of 0.2 g were then added to ~5 g of 2% nitric for ICP-MS analysis. Be, B, Na, Al, P, K, Ca, Sc, V, Cr, Mn, Fe, Co, Ni, Cu, Zn, Ga, As, Sr, Cd, Sn, Sb, Ba, La, Ti, Pb, Bi, Th and U were measured using a Agilent 8900 ICP-MS at Adelaide Microscopy. The results were calibrated against standards HPS-Q17617A (10mg/L Al, As, Ba, Be, Bi, Ca, Cd, Ce, Cs, Co, Cr, Cu, Dy, Er, Eu, Fe, Ga, Gd, Ho, La, Pb, Li, Lu, Mg, Mn, Na, Nd, Ni, P, K, Pr, Rb, Sc, Se, Sm, Sr, Tb, Th, Tl, Tm, U, V, Y, Yb, Zn in 2% HNO3) and ICP-MS68A Solution B (10mg/L Sb, Ge, Hf, Mo, Nb, Si, Ag, Ta, Te, Sn, Ti, W, Zr in HNO3 + trace HF).

3.3.2 Magnetic susceptibility

Magnetic susceptibility is a measurement of the degree of magnetisation in response to an applied magnetic field. For example, a soil sample is made up of many different mineralogical components that each have different magnetic fields and will respond differently when the MS is tested. Magnetic susceptibility is the degree of magnetisation a material acquires in response to an applied magnetic field (Maier et al. 2006:163). Natural and cultural influences such as environment, climate, age, anthropogenic, geogenic and biogenic influences will alter the formation of the sediment, and ultimately its MS value (Dalan 2020:6660; Tite 1972:229). Therefore, magnetism is highly environmentally sensitive.

The ‘magnetic enhancement’ of a sample is a process which will alter the properties of iron minerals and result in enhanced magnetic susceptibility (Dalan and Banerjee 1998:3; Dalan 2020:6660; Tite 1972:229). Minerals are altered within upper sediment layers when magnetic oxides and hydroxides are exposed to high temperatures through fire or pedogenesis (the process of soil formation) (Dalan and Banerjee 1998:3; Dalan 2020:6660; Tite 1972:229). While magnetic enhancement can occur through natural fires, it is particularly relevant in archaeology as it can suggest evidence of human-induced burning (e.g., Lowe and Wallis 2020).

By heating soil samples in nitrogen-then-air to duplicate the effect of fire, Tite and Mullins (1971) verified that MS is enhanced by temperatures of 450°C and above. When studying an archaeological site that has altered levels of MS through the repeated and deliberate use of fire, one can infer the extent of occupation and the degree in which fire was used (Tite and Mullins 1971:219).

All samples from SQ4 and SQ6 (2 cm increments) were measured using a Bartington MS2 Susceptibility System with a MS2B sensor. Samples 8-10, 62- 64, 80-82 and 158-160 cm were missing from the assemblage. The sediment was not sieved prior to analysis but care was taken to exclude smaller debris such as rock fragments to avoid incorrect measurements. Approximately 20 g of sediment was placed in plastic vials and weighed before being measured at low and high frequencies. Each sample was measured three times and the average was used as the final measurement.

3.3.3 Particle size analysis

Particle size analysis provides insight into depositional processes within the rockshelter. It is useful for understanding past climate conditions; for example, an increase in fine-grained sediment could indicate an increasingly windy climate, or coarse grains may suggest internal disintegration of the rock shelter caused by harsh conditions.

Smaller, granule to silt sized particles can be measured using the dry sieving method (Boggs 1987:109; Goldberg and Macphail 2006:338). This method measures the dimension of a grain by using various sieve segments (Boggs 1987:108; Reitz and Shackley 2012:149). The sample is fragmented into numerous size fractions depending on grain diameter and then weighed to find the percentage of each size fractions within a sample (Pye and Blott 2004:19).

For this thesis, participle size was characterised using the most common classification method, the Udden-Wentworth scale (see figure 4) (Boggs 1987:107; Karkanas and Goldberg 2018:24; Leeder 1982:36). This scale sorts the sediment into four major groups based on particle size – clay, silt, sand and gravel – that can then be subcategorised in further detail as shown in figure 4. Grain size is dependent on the velocity of the transporting mechanism, but aeolian systems are generally only capable of transporting very fine sand sized grains and smaller. Grains finer than 100 µm (micrometres) are more susceptible to wind suspension and transport, unlike particles coarser than 1 mm which are typically deposited by strong winds as (Karkanas and Goldberg 2018:64; Reading 2009:15; Visher 1969:1078).

Grain size analysis was conducted using the mechanical dry-sieving method. Samples at 10 cm increments were sieved on a mechanical shaker using an Endecotts precision analytical sieve for approximately 300 seconds using 4.0 mm, 2.0 mm, 1.0 mm, 500 µm, 250 µm, 125 µm and 63 µm sized sieves. The 10-12 cm sample for SQ4 was used instead of 8-10 cm. The sediment remining in each individual sieve was weighed using a precision scale accurate to 0.001 g. The grain size was then calculated using the variation in weight between each size fraction and then classed accordingly using the Wentworth scale.

A limitation of this method is the inability to differentiate sediment finer than 63 µm. Laser granulometry would have enabled further analysis of the types of clay/silt present in the samples (Pye and Blott 2004:19) but was not available at Flinders University during the time of analysis. Therefore, sediment smaller than 63 µm were grouped under a single silt/clay category and was not further analysed.

Figure removed due to copyright restriction

Figure 5 Wentworth grain size classification scale used for the particle size analysis, sourced from Boggs (1987).

3.3.4 Particle shape analysis

Once a general picture of Mertenhof's sedimentological matrix was inferred, it was decided that particle shape analysis would be beneficial. The angular and sphericity of a grain can reveal the transport and depositional history of the sediment.

One downfall when using this method on sand-sized particles is the hardness and durability of quartz. Clastic sediment usually has a high percentage of quartz grains (Leeder 1982:11) that are not modified to the same extent as larger sized grains (such as pebble-cobble) during transport, and are generally only slightly modified, if at all (Boggs 1987:127; Goldberg and Macphail 2006:17). However, this method was successfully utilised to determine the extent to which particle shape changed with depth and enable a comparison between the two squares, and where the sediment originated from – within the cave or from outside sources.

Particle shape consists of three main aspects, the form, roundness, and surface texture of a grain particle (Boggs 1987:123; Leeder 1982:41.) Since these aspects operate as individual properties and can vary without affecting each other, surface texture was not examined due to the reasons discussed above. Roundness refers to the angularity of a grain, specifically the jaggedness, sharpness or roundness of the corners (Boggs 1987:123; Goldberg and Macphail 2006:17; Leeder 1982:41). Sphericity is measured by the extent of a grain's elongation, ranging from a disk-like shape to equant in diameter (Boggs 1987:123; :17; Leeder 1982:41).

These two aspects were classed using the particle shape chart shown in Figure 5. This chart characterises sphericity into three variations of grain sharpness - low, medium and high (see Figure 5). And six variations of roundness – Very Angular, Angular, Sub-Angular, Sub-Rounded, Rounded and Well Rounded (see Figure 5). The analysis was conducted on all samples in the Microarchaeology Laboratory at Flinders University using a zoom stereo microscope.

Figure removed due to copyright restriction

Figure 6 Sphericity chart used to calculate grain shape, sourced from Leeder (1982).

3.3.5 Loss on ignition

Heating minerals to controlled temperatures identifies percentages of organic matter and carbonate material in soil samples. Once moisture is completely removed from the sample two heating steps are required; temperatures of 550ºC will remove organic matter and 1000ºC to remove carbonate material (Heiri et al. 2001:101; LaCcore 2013:2; Schulte and Hopkins 1996:21). Weighing the sample before and after each heating episode will provide the percentage of ignition for each mineral and a basic calculation of the soil composition can be made (Dean 1974:242; Heiri et al. 2001:101-2; LaCcore 2013:2; Schulte and Hopkins 1996:21; Smykatz-Kloss 2012:1).

Following the Loss-on-Ignition Standard Operating Procedure (2013), LOI analysis was performed on sub-samples from all sections at 10 cm intervals. Misplacement of the SQ4 8-10 cm sample meant 6-8 cm was used instead. Approximately 12 g of sediment for each sample was placed in crucibles and weighed before the first heating step was conducted. All measurements were taken using a precision scale. To remove excess moisture the samples were placed in a drying oven at 105ºC and heated overnight for approximately 24 hours. The dry sample weights were recorded and then placed in a muffle furnace for 4 hours at 550ºC to remove organic matter. Once reweighed the muffle furnace was used again at 1000ºC for 2 hours to remove carbonates. The weight difference between each step provides the percentage of matter for each of the three components. To reduce the absorption of atmospheric moisture the samples were measured quickly and systematically placed back in the oven for each heating step. The samples were discarded after the process was completed.

CHAPTER FOUR: RESULTS

4.1 Introduction

The results show at least three different periods where sediment deposition changed over a >150 ka period. The MS shows these events the most distinctly and is supported by the grain size and shape results. These events occur in the form of three distinct changes in results that happen notably around the first 40 cm, the middle 40-92 cm and last 92-160 cm.

4.1.1 Magnetic susceptibility

The MS results are highly variable across both squares.

The frequency dependence results for SQ4 averaged a mean value of 4% (as shown in Figure 6) which typically signifies a dominance of non-superparamagnetic grains or grains finer than 0.005µm (Dearing et al. 1996). Samples between 0-42 cm (<42 ka) display the smallest variability, averaging between 6-7%. Low values were recorded between ~51-54 ka (0.5-2.9% with an outlier of 5.7%), and slight variation between ~54-73 ka (2-4.7%). The lower units (samples 110-158 cm) record four peaks of high values (114-116 cm-9%, 136-138 cm-12%, 140-144 cm-7%, 148-154 cm- 5-6%), all preceded by low frequency dependence (average values <4%).

The high and low frequency magnetic susceptibility results for SQ4 (as shown in Figure 6) have a mean value of 1.04×10^{-7} (LF) and 9.99×10^{-8} (HF). The LF and HF follows the FD results reasonably closely, however discrepancies are noticed within the bottom section. High fluctuation for FD values are matched by low magnetic enhancement after 54 ka. The FD records four peaks of high dependence (114-116 cm - 9%, 136-138 cm - 12%, 140-144 cm-7%, 148-154 cm - 5-6%), these individual samples retain low LF (mean average 6.22×10^{-8} and HF (mean average 5.75×10^{-8}) readings. Contrary to the FD values, the bottom section (samples 110-158 cm) shows little fluctuation between high and low magnetic enhancement, recording the lowest enhancement in the sequence (with a mean LF of 1.00 x 10-7 and HF of 9.66 x 10-8).

High LF and HF values occur within the top 0-40 cm (<41 ka). Readings are strongest between 0-26 cm (mean average LF 2.43×10^{-6}, HF 2.27×10^{-6}), apart from sample 2-4 cm which records the third highest reading of 3.84×10^{-6}. LF and HF starts to decline from 22 cm, starting from LF 2.05×10^{-6} and HF 1.89×10^{-6} and dropping to LF 6.85×10^{-7} and HF 6.56×10^{-7} by 36 cm. A peak of high frequency values is recorded between 38-44 cm (LF 1.98×10^{-6} and HF 1.93×10^{-6}, LF 1.46×10^{-6} and HF 1.37×10^{-6},
1.97×10^{-7}, ~41-52 ka) than proceeded by lower HF and LF values between 44-62 cm (

Values start to increase again between 66 and 72 cm (0.43-1.24%). Samples 74-76 and 76-80 cm (~52 ka) record the highest enhancement almost six times the average mean value (5.15 and 5.13%), then proceeded by extremely low enhancement (0.003-0.035%) for the bottom section (92-160 cm).

Frequency dependence for SQ6 also averaged 4% (as shown in Figure 7) but displayed greater continuity than SQ4, and values below 4% are less common. The top 0-40 cm (<21 ka) fluctuate between 3-6%. The highest overall values are in samples 4-14 cm, displaying consistency between 5-6%. Between 44-60 cm (~21-35 ka) values remain at a constant level of 4%. Slight fluctuation (5-3%) begins between samples 62-80 cm, dropping to 2% for samples 76-80cm (~39 ka). Samples 82-116 cm display the most variability (2-6%) for SQ6, but fluctuations are still continuous. Consistency returns in the bottom samples (118-144 cm) remaining between 4-5%, excluding sample 140-142 cm (1%).

The high and low frequency magnetic susceptibility results for SQ6 (as shown in Figure 7) have a mean value of 1.54% (LF) and 1.47% (HF). The highest enhancement is displayed within the first 0-24 cm, with LF and HF averaging just above 2.0 except samples 14-16 (LF 3.48, HF 3.31) and 18-20 (LF 3.28% and HF 3.11). Samples 20-24 record a sudden spike, reaching the highest values at LF 10.09 and HF 10.06 and LF 4.78 and HF 4.64. Samples 26-40 drop to an average of LF 1.48 and HF 1.41. Samples 44-62 cm are slightly more variable reaching as high as LF 2.91 and HF 2.79 in 42-44 cm and as low as LF 1.46 and HF 1.39 in sample 50-52 cm. An average low of 0.5 is observed between 66-78 cm, slightly rising to an average of 1.12 between 82-124 cm. The bottom 128-144 cm experiences another low of 0.3.

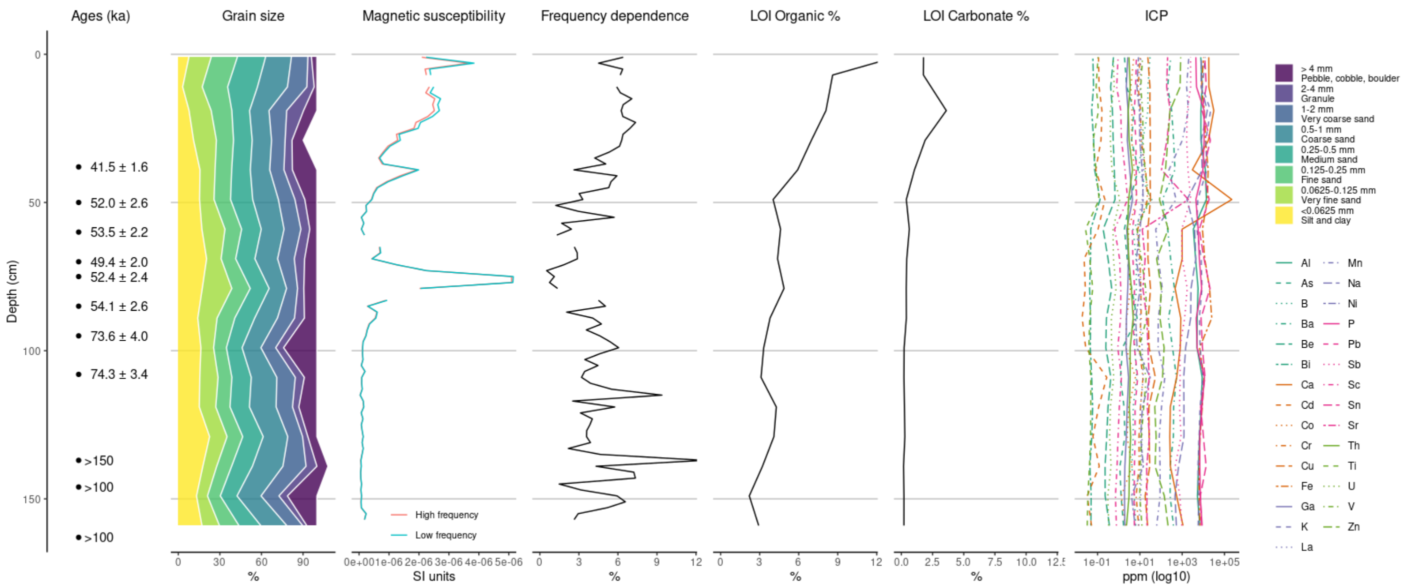

Figure 7 Plot of grain size, MS, LOI and ICP results for SQ4.

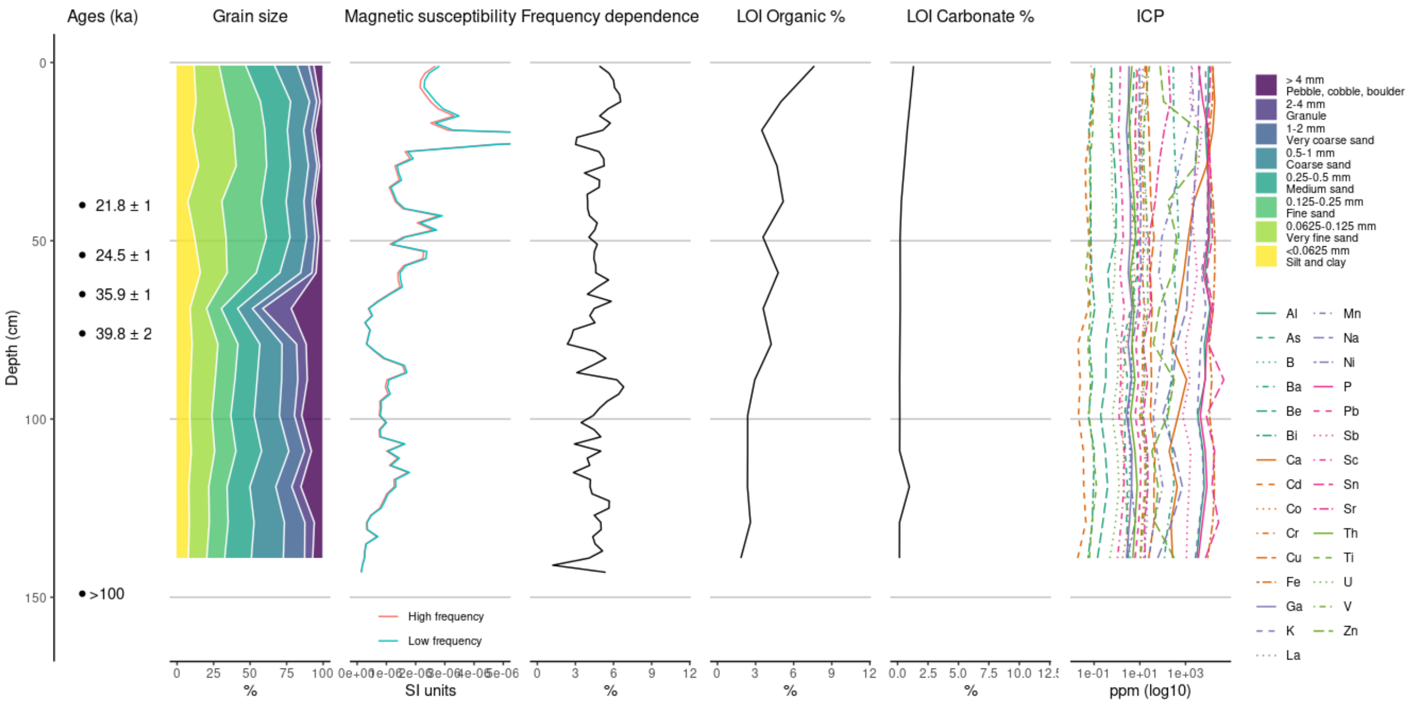

Figure 8 Plot of grain size, MS, LOI and ICP results for SQ6.

4.1.2 Loss on ignition

The LOI results for SQ4 averaged a mean value of 5.16% organic matter, ranging between 2.20 and 13.4%. Carbonate content averaged a mean value of 0.81% and ranged between 0.17 and 3.06%. Both elements decline in a linear way, baring a few outlying samples. High organic and carbonate content occurs between 2-40 cm (~41 ka), ranging between 5.92 and 13.4% (organic) and 1.04 and 3.60% (carbonate). Sample 18-20 cm records the highest carbonate at 3.60%, almost three times the average mean value (organic – 8.09). Both elements decline from 50-110 cm (52-74 ka), ranging between 3.10 to 4.87% organic and 0.20 and 0.63% carbonate. Organic matter increases slightly in samples 118-20 (4.27% organic and 0.24% carbonate) and 128-130 (4.09% organic and 0.27% carbonate), then declines in the last 30 cm (138-140 cm: 3.21, 0.17; 148-150: 2.20%, 0.20%; 158-160 cm: 2.92%, 0.20%).

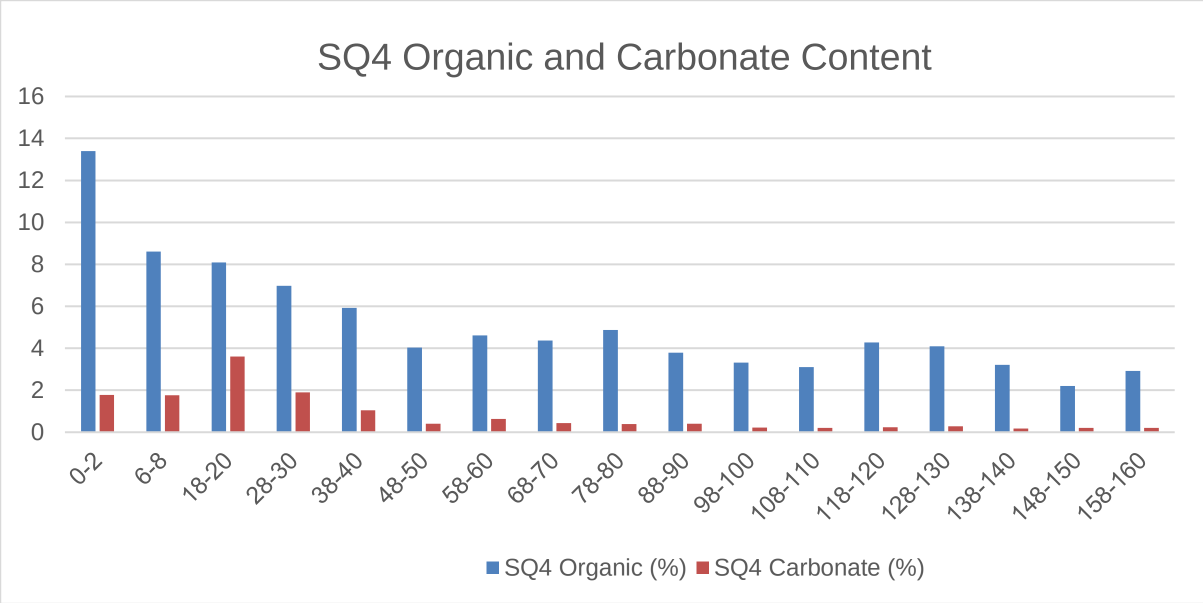

Figure 9 Graph of organic and carbonate content, SQ4.

In SQ6 organic content averaged a mean value of 3.77% and ranged between 1.84 and 7.62%. Carbonate content averaged a mean value of 0.44%, ranging between 0.153 and 1.31%. The top 0-40 cm exhibits the highest organic and carbonate content, but organic matter does not decline in a linear way as per SQ4. Sample 0-2 holds the highest percentage of both elements (7.62 and 1.31%). Organic declines slightly from sample 8-20 (4.99 and 3.48%), then spikes back up between samples 28-40 (4.68 and 5.17%). <21 ka) organic matter drops again at 48-50 cm (3.58%) then increases to 4.78 (sample 58-60), decreases to 3.60% (sample 68-70 cm), and rises again at 78-80 cm (4.23%). The base samples (88-140 cm) average just above 2%, falling to 1.84% at 138-140 cm. While organic matter fluctuates slightly, carbonates gradually decline from 1.31 to 0.15% between 0-2 to 140 cm. Sample 118-120 cm experiences a jump in carbonates (0.96%) almost relative to the top samples but then declines back to 0.16% in the preceding sample (128-130 cm).

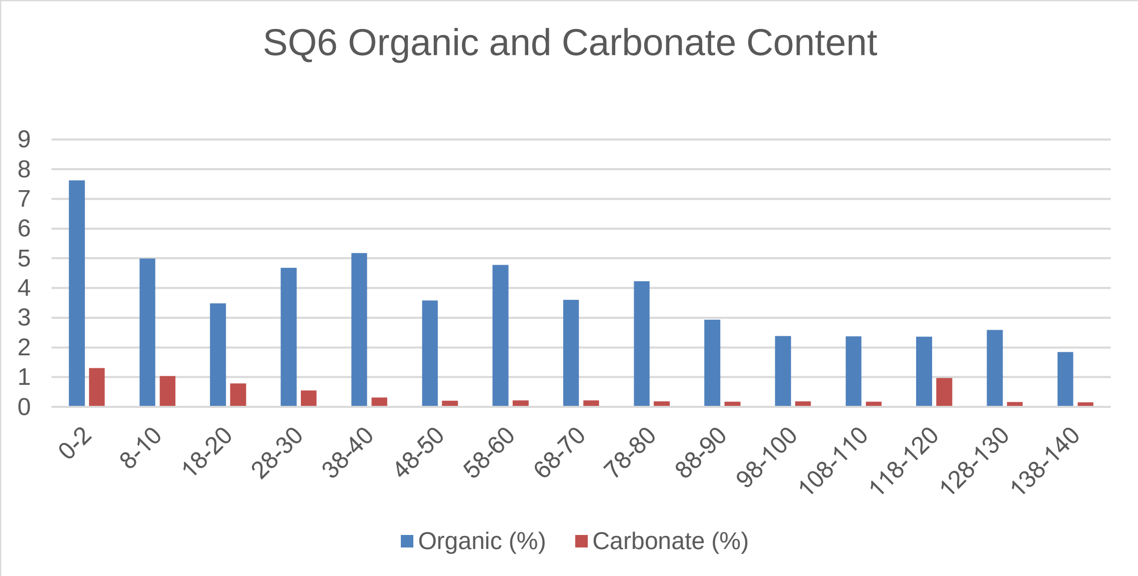

Figure 10 Graph of organic and carbonate content, SQ6

4.1.3 Grain size

The mean grain size for SQ4 was 0.5 µm (Medium Sand) which made up 16.09% of total grains for this square. High levels of sediment finer than <0.5 µm is observed within sample 0-2 cm (0.5 µm: 18.66%; 0.25 µm: 20.34%; 0.125 µm: 18.88%; 0.063 µm: 16.09%) and 10-12 cm (0.5 µm: 21.60%; 0.25 µm: 21.51%; 0.125 µm: 18.38%; 0.063 µm: 14.12%), excluding the clay/silt grouping which retained the lowest numbers for the assemblage (0-2 cm: 7.59%, 10-12 cm: 3.12%). These samples retained some of the lowest granule (4mm) and very coarse (2 mm) grains (0-2 cm: 3.91 and 2.58%; 10-12 cm: 1.95 and 5.27%). Between 18-30 cm granule (4mm) and very coarse (2 mm) grains increase to 8-9%, with sample 38-40 cm recording the first large peak in granule (17.6%). Sample 18-20 cm held the highest percentage of very coarse grains (12.1%). All three samples record slight variation within the 1mm (9-12%), 0.5 µm (13-14%), 0.25 µm (12-13%), 0.125 µm (11-14%), all of which are markedly lower than the overlying top 12 cm. Silt/clay increases from 7.74% at 18-20 cm to 10.9 (28-30 cm) and 15.6% (38-40 cm). The next three samples (48-50 cm, 58-60 cm and 68-70 cm) show slight increases in 1 mm (11-12%), 0.5 µm (16-18%), 0.25 µm (13-15%), and 0.125 µm (11-12). Granule declines to 8.7% at 48-50 cm, declines again to 5.13% at 58-60 cm and then increases back to 8.87% for sample 68-70 cm. Coarse silt declines to ~10% in sample 48-50 and 68-70 cm and jumps back up in the middle sample (58-60 cm) to 16.66%. Clay/silt decreases slightly to 15.31% (48-50 cm), then increases to 16.99% (58-60 cm) and 20.41% (68-70 cm).

Granule increases slightly at 78-80 cm (9.41%) and 88-90 cm (9.0%). 78-80 cm records low 2 mm (4.50%), 1mm (7.98%) and 0.5 µm (12.55%) fractions, and a small increase in 0.125 µm (13.28%). Coarse silt (0.063 µm) nearly doubles the average mean value (21.34%), and clay/silt declines by around 3% (17.27%). The underlying sample (88-90 cm) has increased values of 2 mm (7.11%), 1mm (12.35%), 0.5 µm (16.41%) and 0.25 µm (14.35%). Grains finer than <0.125 decrease to 12.78% (0.125 µm), 13.92% (0.063 µm) and 14.03% (silt/clay). A substantial influx of granule over twice the mean average (24.04%) in sample 98-100 cm is met by a decrease in fractions finer than <2 mm (2 mm: 5.67%; 1mm: 10.66%; 0.5 µm: 13.6%; 0.25 µm: 11.31%; 0.125 µm: 9.22%; 0.063 µm: 9.17%). Clay/silt increases by 2% (16.29%). Samples 108-110 and 128-120 cm are similar for fractions finer than 0.5 µm (0.5 µm: 18.43% and 19.25%; 0.25 µm: 13.98% and 14.03%; 0.063 µm: 13.2% and 11.86%; Clay/silt: 15.47% and 15.15%) and vary slightly for fractions larger than 1 mm (4 mm: 9.05% and 13.02%; 2mm: 6.52% and 4.56%; 1 mm: 13.34 % and 11.82%). Granule is low between 128-130 cm (6.52%) and 138-140 cm (5.53%). The 2 mm, 1 mm and 0.5 µm are lower in 128-130 cm (3.80%, 10.67% and 17.73%) compared to the upper samples and 138-140 cm (7.39%, 15.76% 20.78%), but higher in fractions 0.25 µm (14.76% and 14.18%), 0.125 µm (11.31% and 10.15%), 0.063 µm (12.60% and 9.45%) and a massive influx of silt/clay (22.57% compared to 16.70%). Fractions finer than 0.5 µm decline in 148-150 cm and increase for 158-160 cm (0.5 µm: 17.32% and 18.73%; 0.25 µm: 12.05% and 15.73%; 0.125 µm: 11.31% and 10.15%; 0.063 µm: 7.90% and 12.60%; Clay/silt: 13.1% and 17.05%). The second largest influx of granule occurs in 148-150 cm (21.25% compared to 7.32% for 158-160 cm) and the 2 mm fraction declines from 6.15% to 2.96% in the basal sample.

The mean grain size for SQ6 was coarse silt, with a mean average of 18.1%.The top 0-60 cm records high levels of sediment finer then <0.125 µm and low coarse material (>0.5 µm). A massive influx of 0.125 µm and 0.063 µm occurs between 10-50 cm, ranging between 20.81 and 27.64%, and 20.94 and 27.91%. Clay/silt varies between 7.38 and 12.98% and represents higher values then samples below 58-60 cm. The 1 mm fraction is consistent at around 5%, the 2 mm ranges between 1.65 to 2.24%, and the 4 mm varies more slightly (2.20 to 5.72%). Sample 58-60 cm marks a small decline in sediment finer than <0.25 (0.25 µm: 16.1%; 0.125 µm: 19.90%; 0.063 µm: 18.39%) and an increase in 0.5 µm (14.2%), 1 mm (7.73%), 2mm (2.79%) and 4 mm (4.84). Clay/silt peaks to the highest level at 15.93%. A standalone decline in fine fractions (<0.5 µm) occurs in sample 68-70 cm, recording the lowest percentages for each fraction (0.5 µm: 10.12%; 0.25 µm: 11.07%; 0.125 µm: 10.10%; 0.063 µm: 11.30%; silt/clay: 8.91%). This decline is matched by large influxes in 4 mm and 2 mm fractions, almost three times the size of both mean average values (2 mm: 19.52% and 4 mm: 21.86%).

The bottom 80 cm records large influxes of 0.5 µm, increasing from 15.17% at 78-80 cm to 21.88% by 138-140 cm. The 1 mm fraction follows the same pattern, increasing from 9.92% from sample 78-80 cm to 14.56% by 138-140 cm. 0.125 µm and 0.063 µm decline with depth (ranging from 12.30 and 14.54% (0.125 µm) and 17.63 and 12.55% (0.063 µm) between 78-80 cm and 138-140 cm) and silt/clay decrease slightly (7.77 and 10.34%). The 2 mm fraction is overall higher in these samples, ranging between 4.81 and 6.57%. Granule (4 mm) increases overall, peaking in samples 98-100 cm (14.67%) and 118-120 cm (15.24%). Excluding those two samples, granule ranges from 6.08 to 11.6%.

4.1.4 Grain shape

Consistencies were observed between the angularity of the grains and the coarsening trend noted in the grain size results. Upon examination of the sediment under the microscope, both squares contained growing percentages of low sphericity and highly angular shaped quartz fragments with depth.

SQ4 had an average angularity of 'Angular' (35) and a sphericity of 'medium' (57). The highest level of grain roundness is in the upper section of SQ4 (Table 7). Between 12-14 to 30-32 cm the grains are medium-sub rounded, then continue with an angular trend with depth. From 32-24 to 56-58 cm angularity fluctuates between 'sub angular' and 'angular' with 'medium' and 'low' sphericity. Grains within sample 98-100 cm (high – angular) and 126-128 cm (high – sub angular) have the highest sphericity.

SQ4

Sample	Sphericity	Angularity	OSL Dates (SGC)
0-2	Medium	Sub Angular	
2-4	Medium	Sub Angular	
4-6	Medium	Angular	
6-8	Medium	Angular	
8-10	—	—	
10-12	Medium	Angular	
12-14	Low	Angular	
14-16	Medium	Sub Rounded	
16-18	Medium	Sub Rounded	
18-20	Medium	Sub Rounded	
20-22	Medium	Sub Rounded	
22-24	Medium	Sub Rounded	
24-26	Medium	Rounded	
26-28	Medium	Sub Angular	

28-30	Medium	Sub Rounded	
30-32	Medium	Sub Rounded	
32-34	Medium	Sub Angular	
34-36	Low	Sub Angular	
36-38	Medium	Sub Angular	
38-40	Medium	Sub Angular	41.5 ± 1.6
40-42	Medium	Angular	
42-44	Low	Angular	
44-46	Low	Angular	
46-48	Medium	Sub Angular	
48-50	Low	Angular	52.0 ± 2.6
50-52	Medium	Sub Angular	
52-54	Medium	Sub Angular	
54-56	Medium	Angular	
56-58	Medium	Sub Angular	
58-60	Medium	Sub Angular	53.5 ± 2.2
60-62	Medium	Sub Angular	
62-64	Medium	Sub Angular	
64-66	Medium	Angular	
66-68	Low	Angular	
68-70	Low	Angular	49.4 ± 2.0
70-72	Low	Angular	
72-74	Medium	Angular	
74-76	Medium	Sub Angular	52.4 ± 2.4
76-78	Low	Angular	
78-80	Medium	Sub Angular	
80-82	—	—	
82-84	Low	Angular	
84-86	Medium	Sub Angular	54.1 ± 2.6
86-88	Low	Angular	
88-90	Medium	Angular	
90-92	Medium	Angular	
92-94	Medium	Sub Angular	
94-96	Medium	Angular	73.6 ± 4.0
96-98	Medium	Sub Angular	
98-100	High	Angular	
100-102	Medium	Angular	
102-104	Medium	Angular	
104-106	Medium	Angular	
106-108	Medium	Angular	74.3 ± 3.4
108-110	Medium	Sub Angular	
110-112	Low	Angular	
112-114	Medium	Angular	

114-116	Medium	Sub Angular	
116-118	Medium	Sub Angular	
118-120	Medium	Sub Angular	
120-122	Medium	Angular	
122-124	Medium	Angular	
124-126	Medium	Angular	
126-128	High	Sub Angular	
128-130	Medium	Sub Angular	
130-132	Medium	Sub Angular	
132-134	Medium	Sub Angular	
134-136	Medium	Angular	
136-138	Medium	Angular	>150
138-140	Medium	Angular	
140-142	Medium	Sub Angular	
142-144	Low	Sub Angular	
144-146	Low	Sub Angular	>100
146-148	Medium	Sub Angular	
148-150	Low	Sub Angular	
150-152	Low	Angular	
152-154	Medium	Sub-Angular	
154-156	—	—	
156-158	Low	Angular	
158-160	—	—	

Table 8 Particle shape results for SQ4 with associated OSL dates.

SQ6

Sample	Sphericity	Angularity	OSL Dates (SGC)
0-2	Low	Angular	
2-4	Low	Angular	
4-6	Low	Angular	
6-8	Low	Angular	
8-10	Medium	Angular	
10-12	Medium	Angular	
12-14	Low	Angular	
14-16	Medium	Angular	
16-18	Medium	Sub Angular	
18-20	Medium	Sub Angular	
20-22	Medium	Sub Angular	
22-24	Medium	Sub Angular	
24-26	Medium	Sub Angular	
26-28	Medium	Sub Angular	
28-30	High	Sub Angular	
30-32	Medium	Sub Angular	
32-34	Medium	Sub Angular	
34-36	Medium	Sub Angular	
36-38	Medium	Sub Angular	
38-40	Medium	Sub Angular	21.8 ± 1.2
40-42	Low	Sub Angular	
42-44	Medium	Sub Angular	
44-46	Medium	Sub Angular	
46-48	Medium	Sub Angular	
48-50	Medium	Sub Angular	
50-52	Medium	Sub Angular	
52-54	Medium	Sub Angular	
54-56	Medium	Sub Angular	24.5 ± 1.4
56-58	Medium	Sub Angular	
58-60	Medium	Sub Angular	
60-62	Medium	Sub Angular	
62-64	Low	Sub Angular	
64-66	Low	Angular	35.9 ± 1.4
66-68	Medium	Sub Angular	
68-70	Medium	Sub Angular	
70-72	Medium	Angular	
72-74	Low	Angular	
74-76	Low	Angular	39.8 ± 2.2
76-78	Medium	Sub Angular	
78-80	Low	Angular	
80-82	Low	Angular	
82-84	Low	Angular	
84-86	Medium	Sub Angular	
86-88	Low	Sub Angular	
88-90	Low	Angular	
90-92	Low	Angular	
92-94	Low	Angular	

94-96	Medium	Angular
96-98	Medium	Angular
98-100	Low	Angular
100-102	Low	Angular
102-104	Low	Angular
104-106	Low	Angular
106-108	Medium	Angular
108-110	Low	Angular
110-112	Low	Angular
112-114	Low	Angular
114-116	Medium	Angular
116-118	Low	Angular
118-120	Medium	Angular
120-122	Medium	Angular
122-124	Low	Angular
124-126	Low	Angular
126-128	Low	Angular
128-130	Low	Angular
130-132	Medium	Angular
132-134	Low	Angular
134-136	Low	Angular
136-138	Low	**Very Angular**
138-140	Low	**Very Angular**
140-142	Low	**Very Angular**
142-144	Low	**Very Angular**

Table 9 Particle shape results for SQ6 with associated OSL dates.

SQ6 displayed the same average particle shape as SQ4 - ‘angular’ (39) and ‘medium’ (36) sphericity. No sub angular or round grains were observed (Table 8). 0-2 to 14-16 cm is characterised by ‘angular’ grains with low to medium sphericity. The angularity becomes sub angular from 16-18 to 68-70 cm, then from 70-72 to 86-88 cm fluctuates between angular and sub angular, with low to medium sphericity. Grains are angular with low-medium sphericity from 88-90 to 134-136 cm, changing to very angular/low sphericity for the basal units (136-138 to 142-144 cm).

4.1.5 ICP elemental analysis

In SQ4, the ICP elemental analysis revealed high concentrations of seven principal elements: Calcium (Ca) with a mean average of 18571 ppm, Tin (Sn) averaging 11590 ppm, Iron (Fe) at 11318 ppm, Potassium (K) 8904 ppm, Phosphorus (P) 7303 ppm, Sodium (Na) 4093 ppm, and Aluminium (Al) 7206 ppm. The highest concentration of these elements occurs within the first 50 cm (Table 9).

Element	Average for 0-50 cm (ppm)	Average for 58-160 cm (ppm)
Ca	51433	646
Sn	140391	10254
Fe	12420	10718
K	12719	6824
P	7458	7218
Na	8251	1824
Al	9662	5867

Table 10 comparing the averages for the first 50 cm and the lower 58-160 cm, showing higher values for the top 0-50 cm compared to 58-160 cm in SQ4.

Ca averaged the highest and retained the highest levels in sample 0-2 cm (18066 ppm), 10-12 cm (18239 ppm), and 18-20 cm (31089 ppm). Concentrations drop between 28-30 cm (17398 ppm) and 38-40 cm (3032 ppm), and then increase considerably in sample 48-50 cm (220775 ppm). K remains between 8911 ppm and 14660 ppm for samples 0-12 cm and 28-40 cm. Concentrations rise slightly for 18-20 cm (22053 ppm) and drop as low as 5428 ppm for 58-60 cm. Sn increases at

28-30 (21423 ppm) and 48-50 cm (18718 ppm), averaging 11023 ppm between 0-20 cm and sample 48-50 cm. Fe, Al, and Na remain between 8174 and 16825 ppm. Phosphorus is lower in samples 0-2, 10-12 and 48-50 cm (averaging 4526 ppm), increasing slightly between 18-40 cm (averaging 10390 ppm).
Fe remains higher between 58-120 cm (excluding sample 98-100 cm (6652 ppm) then drops between 7043 and 6250 ppm for the basal units (128-160 cm). P fluctuates between 5658 and 11302 ppm between 60-80 cm and 108-160 cm, declining slightly between 88-100 cm (4602 and 5079 ppm). From 58 cm K remains steady between 4927 and 7022 ppm, expect samples 68-70 (7904 ppm), 78-80 cm (8661 ppm) and 108-110 cm (9583 ppm). Na is higher between 68-90 cm (3852 and 2512 ppm) then drops between 1454 and 457 ppm between 98-160 cm. Aluminium is lower in 58-100 cm (3371 and 5610 ppm) compared to 108-160 cm (5241 and 8833 ppm). Sn fluctuates the highest - peaking slightly in samples 68-70 cm (10723 ppm), 78-80 cm (20593 ppm), 98-100 cm (9099 ppm), 100-110 cm (11954 ppm), 128-130 cm (10084) and 138-140 cm (13423). Calcium also fluctuates between low and high values but remain low compared to the top 50 cm. High values are between 58-60 and 68-70 cm (993 ppm and 1000 ppm), 88-90 and 98-100 (855 and 813.6 ppm), and again at 58-60 cm (1091 ppm). The samples in-between vary between lows of 541 and 260 ppm.

Heavy metals such as manganese (Mn, mean average 1232 ppm), copper (Cu, 29 ppm), cobalt (Co, 4 ppm), nickel (Ni, 10 ppm) and zinc (Zn, 393 ppm) are high in the first 60 cm. Chromium (Cr), Fe, Co, Ni, Cu and gallium (Ga) spike in samples 48-50 cm and 58-60 cm (Cr - 18 ppm and 22 ppm, Fe - 16825 ppm and 15440 ppm, Co - 5 ppm and 7 ppm, Ni - 12 ppm and 30 ppm, Cu - 14 ppm and 31 ppm, Ga - 3 ppm and 4 ppm). A small spike in Cr (13 ppm), Fe (10699 ppm), Co (6 ppm) and Ga (2 ppm) occurs in 118-120 cm while Ni and Cu reach heights of 30 ppm and 53 ppm.

The main elements throughout SQ6 are tin (Sn) (mean average 15325 ppm, iron (Fe) (mean average 14630 ppm), aluminium (Al) (mean average 7661 ppm), phosphurus (P) (7441), and potassium (K) (mean average 6262 ppm), similar to SQ4. Ca remains high within the first four samples (0-30 cm), then declines to 2327 and 192 ppm from 38-140 cm. K is higher withing the top samples between 0-50 cm (7552 and 9304 ppm) dropping to 2660 and 6230 ppm, excluding sample 68-70 which increases to 7876 ppm. P is highest in samples 18-50 cm (averaging 9644 ppm), 68-90 cm (between 13118 and 7035 ppm) and 108-120 cm (7309 and 8552 ppm). Samples in-between fall as low as 3626 and 5877 ppm. Al is higher in the top 70 cm (11765 and 7298 ppm), and lower from 80-140 cm (3091 and 7314 ppm). Fe fluctuates between 9263 and 19117 ppm, with the highest values occurring between 38-70 cm (19117 and 15946 ppm) and 108-130 cm (18263 and 15419 ppm). Sn is consistent for the first 50 cm (9282 and 14915 ppm), then fluctuates between high and low values. Sample 88-90 experiences a massive increase to 46976 ppm, and sample 128-130 cm increase to 27820 ppm. The samples in-between fluctuate between 7394 and

18591 ppm. Na remains strong until 40 cm (2350 and 4178 ppm), then decreases to 60 and 1673 ppm from 50-140 cm.

Heavy metals such as Co (mean average 5 ppm), Ni (9 ppm), Fe (15421 ppm) and Cr (13 ppm) are highest in the first 70 cm. Mn is highest in the first 40 cm (mean average 1200 ppm). Cr (16 ppm, 16 ppm and 12 ppm), Fe (17376 ppm, 18263 ppm and 15419 ppm), Cu (46 ppm, 41 ppm and 41 ppm), and Ga (4 ppm, 4 ppm and 3 ppm) spike again in samples 108-110 cm, 118-120 cm and 128-130 cm.

CHAPTER FIVE: DISCUSSION

5.1 Introduction

The geoarchaeological analysis of Mertenhof indicates that sedimentation in this rock shelter was influenced by a range of climate events, both on large and small scales. These results are similar to other Western Cape sites as well as the local paleoenvironmental data. The three main trends observed in the MS and grain size results are linked to changes in MIS stages – specifically the MIS 2/3 transition, MIS 3/4 transition and MIS 4/5. During the MIS 2/3 transition, there is a notable shift from fine to coarse grains, accompanied by a change in particle shape to more angular and less rounded forms. A decline in aeolian deposition from the LGM to MIS 3 is suggested by low MS and FD levels and the ICP-elemental results. The dry and windy conditions of MIS 3 and the transition to MIS 4 is evident from a small decrease in MS values and a spike in FD. Occupation during MIS 3 is supported by high MS values and low FD. Low MS, varied FD, angular particle shape and four influxes of granule sized sediment (4mm) describes a period of intensified internal erosion brought on by the harsh environmental conditions of MIS 4, possibly continuing into MIS 5.

5.1.1 Magnetic susceptibility

The magnetic mineral results for SQ4 identified three major shifts in magnetic enhancement that compare with small climate fluctuations and changes in MIS stages. Numerous sites throughout South Africa identify similar results, associating the primary cause to major climate events (eg: Herries 2006; Herries 2009; Reidsma et al. 2021).

A substantial shift in the magnetic character of the sediment occurs from the bottom of the sequence (160 cm) to 92 cm bracketed between >100 ka and 54-73 ka. MS values are low and FD becomes significantly varied, reaching peaks of 9 and 12% in places where MS values are low. Similar observations at Sibudu Cave and Rose Cottage Cave have associated an underlying climate trend to these results (Herries 2006; Herries 2009). Low magnetic values were recorded for both sites throughout MIS 4; the cause of such was attributed to an increase in diamagnetic and paramagnetic material produced by internal erosion, and a decrease in the input of fine ferrimagnetic grains (Herries 2006:141-142; Herries 2009:242).

Depending on the lithology of the host bedrock, material derived from the internal disintegration of the rock shelter (e.g., roof spall and erosion) affects the magnetic signature of the soil (Herries 2006:134-135; Herries 2009:236). Diamagnetic minerals (such as quartz and sandstone) can effectively 'dilute' this signature, causing the above pattern of low magnetic readings and reduced fine ferrimagnetic grains (Herries 2006:132, 134; Herries 2009:242; Herries and Fisher 2010:316). Hence, the results at Mertenhof indicate a time of increased internal erosion caused by the harsh glacial conditions of MIS 4, in accordance with both Sibudu and Rose Cottage Cave. Samples with high levels of granule (4 mm) (98-100, 118-120 and 148-150 cm) as indicated in the grain size results also correspond with a higher FD and a low LF and HF reading. Considering the site was occupied (although intensity was reduced significantly - early MSA = 339 total artefacts; SB = 444 total artefacts, (Will et al. 2015:13) during this time a combined anthropogenic component is also possible (Lowe and Wallis 2020).

A distinct change in mineral characteristics occur during the MIS 4/3 transition and continues into MIS 3, also evident at Sibudu and Rose Cottage Cave (Herries 2006; Herries 2009). A strong anthropogenic signal is also observed that has obscured the climate component, but a general increase in signal is still observed during this period. For example, from 90-84 cm a slight increase in MS values may represent the transition from MIS 5 to MIS 4.

Between 80-70 cm MS values are almost double that of the second highest reading, and FD declines. Relatively high MS usually indicates that the material has undergone a chemical alteration caused by the heat from multiple combustion features (Tite and Mullins 1971; Herries and Fisher 2010). An experiment conducted by Herries and Fisher (2010) tested the magnetic signature of experimental fires on local South African cave and dune sand at Pinnacle Point 13b. The results showed that four separate fires were required to enhance the MS values to high proportions and correlated with a decrease in FD values (Herries and Fisher 2010:310). This is a magnetic signature that is unique to South Africa and is markedly different from other areas of the world (e.g., an increase in both MS/FD readings) (Herries 2006:131; Herries 2009:237). Therefore high MS values and medium-low FD is a unique signature that may indicate South African in situ hearths and identify the degree of onsite burning and the intensity of long-term occupation (Herries and Fisher 2010:310; Marean 2010:438). The anthropogenic signature suggested by Mertenhof's MS results is supported by an increase in artefact density as provided by Will et al. (2015) suggesting a time of intense occupation (HP = 2561 total artefacts and post-HP = 3227 total artefacts).

During the first stages of MIS 3 (after the high anthropogenic component) MS values decrease to lows similar to MIS 4 and correspond with a spike in FD (62-52 cm, bracketed between 53-52 ka). This is characteristic of a dry and windy period, although artefact density does not decrease to similar levels as MIS 4 (49 ka = 702 total artefacts and 40 ka = 782 total artefacts) (Will et al. 2015:13).

Fine-to ultra-fine-grained ferrimagnetic grains and higher MS values dominate the top 44 cm. This section is bracketed by a date of 41.5 ka, spanning the Holocene, LGM and MIS 3 transition. Dating is unavailable to refine small oscillations in magnetic values and associate them with a specific climate period, but the results support the general understanding of the paleoclimatic data for the region.

The elevation in fine ferrimagnetic grains and MS values at Mertenof are not characteristic of a typical glacial period that experienced low MS values (Herries 2006; Reidsma et al. 2021). Rose Cottage Cave (located outside of the Western Cape in the Free State) is a good example, recording its lowest MS values within the LGM samples, specifically between 20-14 ka (Herries 2009:242).

The high FD values at Mertenhof reflects the input of aeolian derived sediment, as supported by the grain size and shape results. The Western Cape experienced a cold and wet LGM with large scale aeolian deposition (Chase and Meadows 2000; Chase and Thomas 2007; Meadows and Baxter 1999; Parkington et al. 2000; Scott and Woodborne 2007b). This interpretation is supported by the introduction of fine ferrimagnetic grains associated with aeolian derived sediment (Herries 2006; Herries 2009). The intensity of site use may explain the higher MS results. Lithic density was higher than the MIS 4 deposits at 41 ka (total artefacts = 782), increasing around 22-16 ka (total artefacts = 1043) and declined slightly to 572 at <2ka (Will et al. 2015:13). Anthropogenic enhancement is noted in sample 2-4 cm (high MS and low FD).

MIS Stages	LF Value (Mean average)	Age	Environmental Conditions.
>MIS 5	0.14	>150-74 ka	Cold stadial conditions and increased internal erosion.
MIS 4/3 transition	1.20	~75-74 ka	Slight increase possibly associated with MIS 5/4 transition.
MIS 3	1.76	~54-41 ka	Dry and windy.
MIS 3/2 transition	1.98	~41 ka	Climate transition from harsh conditions of MIS 3 to cold, wet and windy LGM.
<MIS 2	2.01	<41 ka	Windy LGM conditions and warm Holocene.

Table 11 showing the variation in LF values for significant MIS stages, SQ4.

The relative position of SQ4 and SQ6 is interpreted to be responsible for producing variations within the MS results, but similar responses to climate fluctuations are consistent for both squares. SQ6 shares the same anthropogenic component observed in sample 2-4 cm in SQ4, detectable in sample 10-22 cm for SQ6 (high MS and low FD). The decline and fluctuation in MS from 24-42 cm may represent the hiatus that was placed sometime between 16-22 ka, as inferred by Mackay (2016). Another hiatus is suggested between 22-25 ka where SQ6 records two small, but distinct peaks of MS. Considering this suspected hiatus and the corresponding peaks in FD, these results may be climate related instead of anthropogenic. Following a decline between 35-39 ka, a small peak in MS/FD values reflects the LGM/MIS 3 transition just after 39 ka, as indicated at SQ4 around 41 ka. Between 80-128 cm small variation in MS correlating with random lows of FD may be associated with the occupation of MIS 3 (Will et al. 2015:13). Between 35-39 ka the onset of varied FD values may indicate a change in the input of aeolian deposition.

5.1.2 Loss on ignition

The low concentrations of organic material shown by the LOI were expected given the poor preservation conditions of sandstone rock shelters. These types of shelters support a high level of soil acidity and so is a volatile environment that does not favour the preservation of organic matter (see Lowe and Wallis 2020; Sifogeorgaki et al. 2020). In SQ4 organic matter declines from the MIS 2/3 boundary and throughout MIS 3, falling from 5.92 at 41 ka to 0.39% between 54 and 73 ka. Both squares exhibit a substantial decline in carbonate at 38-40 cm, dating to 41 ka for SQ4 (1.04%) and 21 ka at SQ6 (0.31%).

High organic content can be associated with anthropogenic activities (Sifogeorgaki et al. 2020). At Mertenhof organic matter is overall higher in SQ4. Organic content is also highest during occupation periods (<2 ka – 572 (total artefacts), ~16-22 ka – 1043, ~40 ka – 782, ~49 ka – 702, ~50-55 ka – 876, Post-HP (~58-45 ka) and HP (66-58 ka) – 3227, Post-HP (~58-45 ka) and HP (66-58 ka) – 2561, SB (~77-70 ka) – 444, Early MSA – 339). The substantial increase in occupation during the HP and post-HP is most likely represented in the 1% increase in organic content for samples 118-120 and 128-130 cm (Sifogeorgaki et al. 2020). Artefact density declines after the HP to 444 (SB) and 339 (early MSA) total artefacts (Will et al. 2015:13) and organic matter declines to a mean average of 2.78% (samples 138-160 cm) compared to 5.67% for the upper samples (0-130 cm).

SQ4 shares similar readings to Umhlatuzana rock shelter (KwaZulu-Natal, South Africa) between 30 and 60 ka (Sifogeorgaki et al. 2020). Both shelters have an average of around 4% organic content for this period. Both squares at Mertenhof have a higher organic content for <40 ka than Umhlatuzana (SQ4 average 9.27% and SQ6 4.68% compared to Umhlatuzan's average of 2.2%, Sifogeorgaki et al. 2020:565). At Umhlatuzan artefacts were low in these layers (Sifogeorgaki et al. 2020:569).

5.1.3 Particle size

The influx of material finer than <0.125 µm for the LGM samples in SQ6 indicate a windy environment in comparison to the MSA. Dates place these samples within the cold, windy and moist conditions of the LGM and the onset of warm and dry Holocene conditions (Chase and Meadows 2000; Chase and Thomas 2007; Meadows and Baxter 1999; Parkington et al. 2000; Scott and Woodborne 2007b). The results from SQ4 before 41 ka follow the same pattern, although these samples remain undated. In SQ6, the two samples dated between ~21-24 ka and the two undated samples above represent the highest levels of sediment finer than 0.125 µm. These samples suggest an increase in aeolian deposition.

The movement of these grains were dictated by the strength of the transporting mechanism (wind). The LGM and Holocene represent a time in which this mechanism was the strongest, and the accumulation rate was the highest than any other period. Considering Mertenhof is situated at a height of ~25 m above the main source of external sediment, it is unlikely that wind could suspend and transport sediment coarser than <0.125 µm and introduce these sizes into the shelter (Karkanas and Goldberg 2018:64; Reading 2009:15; Visher 1969:1078). Fractions larger than this are considered a direct function of internal erosion. Because fine material decreases after the LGM, it is likely that windy conditions prevailed until the end of the LGM and was replaced by erosive processes during the LGM/MIS 3 transition.

A change in the level of depositional energy occurs in both squares between ~30 and 40 ka where the input of material finer than <0.125 µm declines and is replaced by an influx of sediment coarser than <0.5 µm. In SQ4 the upper part of the sequence contains dominant levels of aeolian introduced fine sediment until the end of the LGM. The decline seems to start from here, and by ~40 ka material coarser than <0.125 µm becomes the dominant grain size for both squares. However, SQ4 records a marked increase in the clay fraction (<0.063 µm) that remains this way with depth. One consideration for the lack of particles finer than <0.125 µm is winnowing – the removal of medium and fine-grained sediment by geological processes, e.g., wind or water, leaving behind the coarser particles (Goldberg and Macphail 2006; Karkanas and Goldberg 2018). This may not be the case at Mertenhof because of the increase in silt/clay, and instead may have been driven by the MIS 2/3 transition triggering the beginning of small-scale internal erosion (as supported by the MS/FD results, increasingly angular particle shape and chemical analysis). The low LF and HF readings in the MS is also more supportive of this theory. A change in wind direction could also restrict the introduction of aeolian transport, but further research on paleowind patterns will be needed to explore this possibility further. At this stage with the paleoclimate data that is available and the results from this analysis the lack of particles finer than <0.125 µm seems to be resultant from a decline in windy conditions.

Sometime between the Late MSA (<40 ka) and 35 ka Elands Bay cave recorded two significant roof spall events that reflects a time of sever internal erosion (Porraz et al. 2016:42). Similar to Mertenhof, a decline in coarse material is documented during the LGM between 24-19 ka (Porraz et al. 2016:43). At Die Kelders around 32 ka a low of 11.7°C is associated with a significant roof fall event (Thackery 2002:751).

Between ~100 and 30 ka intense weathering occurred at other Western Cape sites. At Diepkloof, salt induced spalling caused high amounts of sand-sized quartz grains, “plaquettes” and “éboulis” to accumulate between the lower MSA and later intermediate HP (Miller et al. 2013). Closer to Mertenhof, the stratigraphic matrix at Klein Kluphis recorded a consistent and high rate of roof spall throughout 20-65 ka (Mackay 2010). Die Kelders and Diepkloof experienced frost shattering during the MSA (Chase and Thomas 2007:114).

The erosion at Mertenhof is not as extensive as these shelters. However, considering the onset of this coarse material parallels with a characteristically harsh environmental context, the results are interpreted as an increase in internal erosion. The grain size suggests that the dominant depositional processes during the LGM was aeolian. By ~30 ka the strength of this energy declines and is replaced by higher levels of internal erosion from ~30 ka onwards.

SQ4 records three main influxes of granule (>4 mm) sediment after ~40 ka interpreted as higher levels of internal erosion (for example Chase and Thomas 2007; Miller et al. 2013). The smallest of the three is at 41 ka but is still more than double the average percentage (sample 38-40 cm - 17.69%). A significant erosive event during ~73-74 ka (98-100 cm – 24.04% and 118-120 cm – 13.02%) parallels with MIS 5a/4. This transition experienced global sea level transgression between 70-76 ka and a decline in humidity and moisture availability (Mackay and Cartwright 2022:7). Internal disintegration was largely intensified by changes in moisture. Another large influx of granule sized sediment occurs in the lower basal units (148-150 cm – 21.25%, <100 ka) maybe a product of the oscillating cool/warm conditions during MIS 5, or may represent the semi-arid glacial conditions of MIS 6 (Reynard 2021). Further dating will be required to narrow down the exact age and associated environmental context. The MS results support a period of internal erosion based on low LF and HF readings.

5.1.4 Particle shape

The highest level of grain roundness occurs within the upper section of SQ4. Between depths 12-14 to 30-32 cm the grains are medium-sub rounded, then continue with an angular trend with depth. While no dates were obtained for these samples, based on the next available date of ~41 ka at 40 cm it is assumed here that they span the duration of the LGM. It is noted that further dating is required to confirm this assumption.

For SQ6 the particle shape between ~21-24 ka was medium-sub angular which continues both before and after the LGM dated samples. Aside from a few singular cases of medium-sub angular further down the square, this section of SQ6 represents the least angularity throughout the assemblage. Both squares demonstrate the highest level of roundness between the LGM and MIS 3 boundary.

5.1.5 ICP elemental analysis

The ICP analysis revealed high levels of elements in SQ4 that are commonly associated with archaeological sediments (Ca, K, P, Na) (Oonk et al. 2009:38). The highest concentration of elements occurs within the upper 50 cm. The MS/FD and grain size results suggested that during <40 ka aeolian deposition intensified, increasing further during the LGM and Holocene. The increase in these elements may be climate related, resulting from an increase in sediment input from introduced sediment. In both squares higher concentrations of Al, K and Ca and a decrease in grain size for the top 50 cm may suggest an increase in clay associated with heightened aeolian deposition. Around the MIS 2/3 boundary larger concentrations of Ca, Sn and Al compare with a slight increase in FD (48-50 cm) values (increasing from 2.61% to 3.30% and declining to around 1-2% for subsequent samples 68-80 cm). This is probably related to the onset of MIS 2 conditions.

SQ4 recorded the highest concentrations of P and Al between 18-40 cm and 108-160 cm. P is often used as a proxy for site use (Oonk et al. 2009:38). However, the P content at Mertenhof is not the most reliable indication of site use when compared against artefact density. 782 artefacts (Will et al. 2015:13) are associated with the 18-40 cm samples and retained an average P reading of 10390.28 ppm. The density of artefacts and higher P average confirms that occupation intensity was quite high around ~41 ka, but as artefact density increases with depth the average P declines. Nearly 100 more artefacts (876) are found between samples 88-110 cm but average P content is lower (6994.49 ppm). Artefact density is significantly higher in the subsequent 108-160 cm (3227 and 2561 artefacts) but P has a lower average than samples between 18-40 cm of 8218.4 ppm.

Two interpretations could be deduced from these inconstancies. The P element could be interpreted as an unreliable indication of site use, perhaps because of low preservation due to the acidic environment. Or another explanation could be that the total number of artefacts do not portray an accurate description of occupation intensity. The MS reacted to two instances of anthropogenic burning over a >150 ka period. Anthropogenic signals at Mertenhof are generally low so it is possible that the site was not occupied as intensely as the artefact density may suggest.

Mn, Cu, Co, Ni and Zn concentrations are highest in the first 60 cm (<52 ka). Artefact density is between 1043, 782 and 702 (Will et al. 2015:13) so the increase in these heavy elements is most likely fire related. The heavy metal concentrations decrease similar to the P after 120 cm. A large increase in Co, Ni and Cu corresponds with the highest total number of artefacts (3227) (Will et al. 2015:13). However, in the preceding samples where artefact density is still high (2561) (Will et al. 2015:13) there are no major increases in any of these elements and percentages are low. This would suggest that fire was used more frequently before <53 ka where artefact density was generally lower.

P and artefact density follow a closer relationship in SQ6. P and Al are highest in samples 18-50 cm, 68-90 and 108-118 cm when artefacts are generally high (1043) (Will et al. 2015:13). P declines slightly over the 22-24 ka hiatus and then increases again when artefact density rises (782) (Will et al. 2015:13). The higher percentages of heavy metals such as Co, Ni, Fe, Cr and Mn in the first 70 cm of SQ6 may represent a greater level of fire use before 22 ka. Along with the P element, these heavy metals decrease over the 22-24 ka hiatus and increase again when occupation intensifies after 39 ka.

5.1.6 Variation between SQ4 and SQ6

The location within an archaeological rock shelter can impact the sediment properties because the origin, transport and deposition of sediment can be affected by many systems. For example, samples taken from the drip line of a shelter may have a different sedimentary input than sediment from the back of the cave because of the proximity to the cave opening, and is more susceptible to the introduction of aeolian, fluvial and depositional processes.

Both squares show evidence of different depositional processes based on their positions within the rock shelter. This pattern is validated across all the results. When compared to SQ6, SQ4 recorded higher variation in every method that was conducted. This square is located towards the centre of the cave where sediment deposition is observed to be higher and the grain size and MS is less predictable, most likely due to its position closer to the entrance of the cave. Sediment has a higher likelihood of being introduced by aeolian or fluvial processes or anthropogenic activity: human occupation is generally centred towards the middle and entrances where everyday activities can manipulate soil formation. These processes are most likely responsible for the variations between SQ6.

The results for SQ6 were to be expected when considering its position towards the back of the cave. The way the shelter narrows towards the rear would have limited the introduction of sediment and access for occupying humans. Reduced exposure to processes such as weather and human activity would intern decrease the level of introduced anthropogenic and geogenic sediment and would limit the variation in sediment.

5.1.7 Addressing the relationship between artefact density and anthropogenic burning

The MS results suggest that climate had the biggest impact on Mertenhof's sedimentary profile. The presence of other anthropogenic signals (e.g., artefacts) suggest that the site was frequently used. But evidence of anthropogenic burning is generally low and LF and HF spikes only briefly when artefact density is at its highest. A likely explanation for this is that burning was conducted in other areas of the shelter, as observed in Diepkloof (Miller et al. 2013). The excavation squares are situated towards the back of the shelter were burning would be less likely to occur.

CHAPTER SIX: RECOMMENDATIONS FOR FUTURE WORK AND CONCLUSION

6.1 Recommendations for future work

To gain further understanding of the climate mechanisms that have affected the sedimentary deposition at Mertenhof rock shelter it is suggested that additional research be conducted:

- Sedimentary analysis on the remaining excavation squares (SQ1, SQ2, SQ3 and SQ5) would gain further information on site formation processes and identify the impact that different positions within the rock shelter have on sediment deposition.
- Phytolith analysis would create a highly detailed climate reconstruction that could be used as a proxy for paleoclimate.
- A micromorphological analysis would be useful to use in conjunction with the results gained here to investigate other sedimentary characteristics such as grain texture and weathering. This method would help recognise the climate processes that have affected the sediment and add additional details to the deposition process at Mertenhof.

6.2 Conclusion

Subtle changes in the sedimentary matrix of Mertenhof provides insight into the climate conditions of the Western Cape for the last >150 ka. While other proxies suggest cold and windy conditions in the Western Cape during this period, the sediments in Mertenhof responded subtly to these conditions in the form of small-scale erosion and limited introduced aeolian sediment. This relatively stable response indicates that the height above the Beidow River and orientation of the shelter was responsible for reducing sediment input during major climate events. Nevertheless, major climate events from the Holocene, LGM and MIS 3-6 can be interpreted from small- or large-scale variations in sedimentation.

Each set of results support the same underlying climate trends. The MS, ICP elemental analysis and grain size and shape results indicate that a windy climate prevailed until 40 ka based on the correlation of fine ferrimagnetic grains, fine sediment fractions, rounded particle shape and chemical elements commonly found in clay. The Southwestern Cape experienced an unusually windy glacial period during the LGM which is observable in these four results. The decline in fine-grained material, MS and FD values, clay-related elements and increasingly angular particle shape after the LGM suggests that these windy conditions were replaced by erosive processes during the LGM/MIS 3 transition. Conditions most likely deteriorated with age, fluctuating between glacial and interglacial stages and increasing the level of internal erosion within the rock shelter. The MS results proved most valuable in terms of creating a more in-depth view of the environmental mechanisms at play for the later periods. For example, a low magnetic and FD signature during MIS 4 supports the general conditions of this period accurately (harsh glacial conditions with little aeolian input). A slight increase in MS values and an influx of granule (>4 mm) sediment may represent the transition from MIS 4 to MIS 5. The low magnetic and varied FD values during MIS 3 point to a climate where erosion was still caused by harsh conditions, but sediment was introduced into the shelter more frequently by aeolian means. Erosion around <100 ka could have been induced by oscillating cool/warm conditions during MIS 5, or from the semi-arid glacial conditions of MIS 6.

The MS results support evidence for occupation during MIS 3. The results show a clear magnetic signature (high MS and low FD) that is associated with insitu South African hearths between ~50-55 ka. Apart from MIS 3, clear evidence of anthropogenic enhancement is general lacking in all the results conducted here.

References:

Ambrose, S.H. 2002 Small things remembered: origins of early microlithic industries in sub-Saharan Africa. *Archeological Papers of the American Anthropological Association* 12(1):9–29.

Ambrose, S.H. and K.G. Lorenz 1990 Social and ecological models for the Middle Stone Age in southern Africa. In P. Mellars (ed.) *The emergence of modern humans: An archaeological perspective*, pp.3–33. Edinburgh: Edinburgh University Press

Ames, C.J.H., M. Shaw, C. O'Driscoll, A. Mackay 2020b A multi-user mobile GIS solution for documenting large surface scatters: an example from the Doring River, South Africa. *Journal of Field Archaeology* 45(6):394–412.

Ames, C.J.H., S. Chambers, M. Shaw, N. Phillips, B.G. Jones, and A. Mackay 2020a Evaluating erosional impacts on open-air archaeological sites along the Doring River, South Africa: methods and implications for research prioritization. *Archaeological and Anthropological Sciences* 12(5):1–15.

Arroyo-Kalin, M. 2020 Anthropogenic Sediments and Soils: Geoarchaeology. In C. Smith (ed.), *Encyclopedia of Global Archaeology,* pp.425–430. Cham: Springer International Publishing, Department of Archaeology, Flinders University.

Badenhorst, S. and I. Plug 2012 The faunal remains from the Middle Stone Age levels of Bushman Rock Shelter in South Africa. *South African Archaeological Bulletin*, 67(195):16–31.

Barham, A. and G. Huckleberry 2014 Sediments. In J. Balme and A. Paterson (eds), *Archaeology in Practice: A Student Guide to Archaeological Analyses*, pp.86–101. London: Bloomsbury.

Bellwood, P. and I. Ness 2014 *The Global Prehistory of Human Migration*. Chichester: John Wiley & Sons, Incorporated.

Benito, G., V.R. Thorndycraft, M.T. Rico, Y. Sanchez-Moya, A. Sopena, B.A. Botero, M.J. Machado, M. Davis and A. Perez-Gonzalez 2011 Hydrological response of a dryland ephemeral river to southern African climatic variability during the last millennium. *Quaternary Research* 75(3):471–482.

Bluszcz, A. 2004 OSL dating in archaeology. In E.M. Scott, A.Y. Alekseev and G.I. Zaitseva (eds), *Impact of the environment on human migration in Eurasia*, pp.137–149. Series IV: Earth and Environmental Sciences 42. Dordrecht: Springer Science & Business Media, NATO Scientific Affairs Division.

Boelhouwers, J.C. 1999 Relict periglacial slope deposits in the Hex River Mountains, South Africa: observations and palaeoenvironmental implications. *Geomorphology* 30(3):245–258.

Boelhouwers, J.C. and K.I. Meiklejohn 2002 Quaternary periglacial and glacial geomorphology of southern Africa: review and synthesis: Periglacial and Permafrost Research in the Southern Hemisphere. *South African Journal of Science* 98(1):47–55.

Boggs, S. 1987 *Principles of Sedimentology and Stratigraphy*. Columbus: Merrill Publishing.

Brown, K.S., C.W. Marean, A.I. Herries, Z. Jacobs, C. Tribolo, D. Braun, D.L. Roberts, M.C. Meyer and J. Bernatchez 2009 Fire as an engineering tool of early modern humans. *Science* 325(5942):859–862.

Butzer, K.W. 1978 Sediment stratigraphy of the middle stone age sequence at Klasies River mouth, tsitsikama coast, South Africa. *The South African Archaeological Bulletin* 33(128):141–151.

Butzer, K.W. 2004 Coastal eolian sands, paleosols, and Pleistocene geoarchaeology of the Southwestern Cape, South Africa. *Journal of Archaeological Science* 31(12):1743–1781.

Chase, B.M. and D.S. Thomas 2007 Multiphase late Quaternary aeolian sediment accumulation in western South Africa: timing and relationship to palaeoclimatic changes inferred from the marine record. *Quaternary International* 166(1):29–41.

Chase, B.M. and M.E. Meadows 2007 Late Quaternary dynamics of southern Africa's winter rainfall zone. *Earth-Science Reviews* 84(3-4):103–138.
Chase, B.M., S. Lim, M. Chevalier, A. Boom, A.S. Carr, M.E. Meadows and P.J. Reimer 2015 Influence of tropical easterlies in southern Africa's winter rainfall zone during the Holocene. *Quaternary Science Reviews* 107:138–148.
Clarke, R. 2013 *Australopithecus* from Sterkfontein Caves, South Africa. In K. Reed, J. Fleagle and R. Leakey (eds), *The Paleobiology of Australopithecus*, pp.105–123. Vertebrate Paleobiology and Paleoanthropology. Dordrecht: Springer.
Clarke, R.J. 2008 Latest information on Sterkfontein's Australopithecus skeleton and a new look at Australopithecus: research in action. *South African Journal of Science* 104(11):443–449.
Cowling, R.M., C.R. Cartwright, J.E. Parkington and J.C. Allsopp 1999 Fossil wood charcoal assemblages from Elands Bay Cave, South Africa: implications for Late Quaternary vegetation and climates in the winter-rainfall fynbos biome. *Journal of Biogeography* 26(2):367–378.
Dalan, R. 2020 Magnetic Susceptibility of Soils and Sediments in Environmental Archaeology. In C. Smith (ed.), *Encyclopedia of Global Archaeology,* pp.425–430. Cham: Springer International Publishing, Department of Archaeology, Flinders University.
Dalan, R.A. and S.K. Banerjee 1998 Solving archaeological problems using techniques of soil magnetism. *Geoarchaeology: An International Journal* 13(1):3–36.
Deacon, H.J. 1995 Two late Pleistocene-Holocene archaeological depositories from the southern Cape, South Africa. *The South African Archaeological Bulletin* 50(162):121–131.
Deacon, H.J. and J. Deacon 1999 *Human beginnings in South Africa: uncovering the secrets of the Stone Age*. Cape Town: New Africa Books.
Dean, W.E. 1974 Determination of carbonate and organic matter in calcareous sediments and sedimentary rocks by loss on ignition; comparison with other methods. *Journal of Sedimentary Research* 44(1):242–248.
Dearing, J.A., K.L. Hay, S.M. Baban, A.S. Huddleston, E.M. Wellington and P. Loveland 1996 Magnetic susceptibility of soil: an evaluation of conflicting theories using a national data set. *Geophysical Journal International* 127(3):728–734.
Delagnes, A., P. Schmidt, K. Douze, S. Wurz, L. Bellot-Gurlet, N.J. Conard, K.G. Nickel, K.L. Van Niekerk and C.S. Henshilwood 2016 Early evidence for the extensive heat treatment of silcrete in the Howiesons Poort at Klipdrift Shelter (Layer PBD, 65 ka), South Africa. *PloS one* 11(10):1–27.
Dincauze, D.F. 2000 *Environmental Archaeology: Principles and Practice*. Cambridge: Cambridge University Press.
Dusseldorp, G., M. Lombard and S. Wurz 2013 Pleistocene homo and the updated stone age sequence of South Africa. *South African Journal of Science* 109(5):1–7.
French, C. A. I. 2003 *Geoarchaeology in Action: Studies in Soil Micromorphology and Landscape Evolution*. London: Routledge.
Goldberg, P. and R. Macphail 2006 *Practical and Theoretical Geoarchaeology*. Carlton: Blackwell Publishing.
Hall, M. 1996 *Archaeology Africa*. Oxford: James Currey Publishers.
Hassan, F.A. 1979 Geoarchaeology: The geologist and archaeology. *American Antiquity* 44(2):267–270.
Heiri, O., A.F. Lotter and G. Lemcke 2001 Loss on ignition as a method for estimating organic and carbonate content in sediments: reproducibility and comparability of results. *Journal of paleolimnology* 25(1):101–110.
Henshilwood, C.S. 2008 Winds of change: Palaeoenvironments, material culture and human behaviour in the Late Pleistocene (~ 77 ka-48 ka ago) in the western Cape Province, South Africa. *Goodwin Series* 10:35–51.

Herries, A.I. 2006 Archaeomagnetic evidence for climate change at Sibudu Cave. *Southern African Humanities*, 18(1):131–147.
Herries, A.I. and E.C. Fisher 2010 Multidimensional GIS modeling of magnetic mineralogy as a proxy for fire use and spatial patterning: Evidence from the Middle Stone Age bearing sea cave of Pinnacle Point 13B (Western Cape, South Africa). *Journal of Human Evolution* 59(3-4):306–320.
Herries, A.I., J.M. Martin, A.B. Leece, J.W. Adams, G. Boschian, R. Joannes-Boyau, T.R. Edwards, T. Mallett, J. Massey, A. Murszewski, S. Neubauer, R. Pickering, D.S. Strait, B.J. Armstrong, S. Baker, M.V. Caruana, T. Denham, J. Hellstrom, J. Moggi-Cecchi, S. Mokobane, P. Penzo-Kajewski, D.S. Rovinsky, G.T. Schwartz, R.C. Stammers, C. Wilson, J. Woodhead and C. Mente 2020 Contemporaneity of Australopithecus, Paranthropus, and early Homo erectus in South Africa. *Science* 368(6486):1–19.
Herries, A.I.R. 2009 New approaches for integrating palaeomagnetic and mineral magnetic methods to answer archaeological and geological questions on Stone Age sites. In A. Fairbairn, S. O'Connor and B. Marwick (eds), *New Directions in Archaeological Science*, pp.235–253. Canberra: ANH Publications, Department of Archaeology and Natural History, Research School of Pacific and Asian Studies, The Australian National University.
Jacobs, Z. and R.G. Roberts 2007 Advances in optically stimulated luminescence dating of individual grains of quartz from archaeological deposits. *Evolutionary Anthropology: Issues, News, and Reviews: Issues, News, and Reviews* 16(6):210–223.
Jacobs, Z., A.G. Wintle, G.A.T. Duller, R.G. Roberts and L. Wadley 2008 New ages for the post-Howiesons Poort, late and final Middle Stone Age at Sibudu, South Africa. *Journal of Archaeological Science* 5(7):1790–1807.
Jacobs, Z., R.G. Roberts, R.F. Galbraith, H.J. Deacon, R. Grun, A. Mackay, P. Mitchell, R. Vogelsang and L. Wadley 2008 Ages for the Middle Stone Age of southern Africa: implications for human behavior and dispersal. *Science* 322(5902):733–735.
Karkanas, P. and P. Goldberg 2018 *Reconstructing archaeological sites: understanding the geoarchaeological matrix*. Oxford: John Wiley & Sons.
Klein, R.G., G. Avery, K. Cruz-Uribe, D. Halkett, J.E. Parkington, T. Steele, T.P. Volman and R. Yates 2004 The Ysterfontein 1 Middle Stone Age site, South Africa, and early human exploitation of coastal resources. *Proceedings of the National Academy of Sciences* 101(16):5708–5715.
Klein, R.G., G. Avery, K. Cruz-Uribe, D. Halkett, T. Hart, R.G. Milo and T.P. Volman 1999 Duinefontein 2: an Acheulean site in the western Cape province of South Africa. *Journal of human evolution* 37(2):153–190.
Leeder, M. R. 1982 *Sedimentology: Process and Product*. Dordrecht: Springer Netherlands.
Levin, N.E. 2015 Environment and climate of early human evolution. *Annual Review of Earth and Planetary Sciences* 43:405–429.
Lombard, M. 2008 Finding resolution for the Howiesons Poort through the microscope: micro-residue analysis of segments from Sibudu Cave, South Africa. *Journal of Archaeological Science* 35(1):26–41.
Lombard, M., L.Y.N. Wadley, J. Deacon, S. Wurz, I. Parsons, M. Mohapi, J. Swart and P. Mitchell 2012 South African and Lesotho stone Age sequence updated (I). *South African Archaeological Bulletin* 67(195):123–144.
National Lacustrine Core Facility 2013 Loss-on-Ignition Standard Operating Procedure. Retrieved 21 July 2023 from < https://drive.google.com/file/d/1gl0y4H-3xYWnuFL3uDikVWyh6GwKDweI/view>.
Low, M. and A. Mackay 2018 The organisation of Late Pleistocene Robberg Blade Technology in the Doring River Catchment, South Africa. *Journal of African Archaeology* 16(2):168–192.
Low, M., A. Mackay and N. Phillips 2017 Understanding Early Later Stone Age technology at a landscape-scale: evidence from the open-air locality Uitspankraal 7 (UPK7) in the Western Cape, South Africa. *Azania: Archaeological Research in Africa* 52(3):373–406.

Lowe, K.M. and L.A. Wallis 2020 Exploring ground-penetrating radar and sediment magnetic susceptibility analyses in a sandstone rockshelter in Northern Australia. *Australian archaeology* 86(1):63–74.
Mackay, A. 2010 The late Pleistocene archaeology of Klein Kliphuis rock shelter, Western Cape, South Africa: 2006 excavations. *South African Archaeological Bulletin* 65(192):132–147.
Mackay, A. 2011 Nature and significance of the Howiesons Poort to post-Howiesons Poort transition at Klein Kliphuis rockshelter, South Africa. *Journal of Archaeological Science* 38(7):1430–1440.
Mackay, A. 2016 Three arcs: observations on the archaeology of the Elands Bay and northern Cederberg landscapes. *Southern African Humanities* 29(1):1–15.
Mackay, A. and C.R. Cartwright 2022 Coherent changes in wood charcoals, site occupation and lithic technology across the MIS 4/3 transition at Klein Kliphuis rock shelter, South Africa. *Journal of Quaternary Science* 38(1):38–48.
Mackay, A., C.R. Cartwright, S. Heinrich, M.A. Low, M.C. Stahlschmidt and T.E. Steele 2019 Excavations at Klipfonteinrand reveal local and regional patterns of adaptation and interaction through MIS 2 in southern Africa. *Journal of Paleolithic Archaeology* 1-36.
Mackay, A., C.R. Cartwright, S. Heinrich, M.A. Low, M.C. Stahlschmidt and T.E. Steele 2020 Excavations at Klipfonteinrand reveal local and regional patterns of adaptation and interaction through MIS 2 in southern Africa. *Journal of Paleolithic Archaeology* 3:362–397
Mackay, A., E. Hallinan and T.E. Steele 2018 Provisioning responses to environmental change in South Africa's winter rainfall zone: MIS 5-2. In E. Robinson and F. Sellet (eds), *Lithic technological organization and paleoenvironmental change*, pp.13–36. Studies in Human Ecology and Adaptation 9. Cham: Springer, Department of Anthropology, University of Kansas.
Mackay, A., Z. Jacobs, T.E. Steele 2015 Pleistocene Archaeology and Chronology of Putslaagte 8 (PL8) Rockshelter, Western Cape, South Africa. *Journal of African Archaeology* 13(1):71–98.
Maier, G., R. Scholger and J. Schön 2006 The influence of soil moisture on magnetic susceptibility measurements. *Journal of Applied Geophysics* 59(2):62–175.
Marean, C.W. 2010 Pinnacle Point Cave 13B (Western Cape Province, South Africa) in context: the Cape floral kingdom, shellfish, and modern human origins. *Journal of Human Evolution* 59(3-4):425–443.
Mayewski, P.A., E.E. Rohling, J.C. Stager, W. Karlén, K.A. Maasch, L.D. Meeker, E.A. Meyerson, F. Gasse, S. van Kreveld, K. Holmgren and J. Lee-Thorp 2004 Holocene climate variability. *Quaternary research* 62(3):243-255.
McCall, G.S. and J.T. Thomas 2012 Still Bay and Howiesons Poort foraging strategies: recent research and models of culture change. *African Archaeological Review* 29:7–50.
Meadows, M.E. and A.J. Baxter 1999 Late Quaternary palaeoenvironments of the southwestern Cape, South Africa: a regional synthesis. *Quaternary International* 57(8):193–206.
Meadows, M.E. and J.M. Sugden 1990 Late Quaternary vegetation history of the Cederberg, southwestern Cape Province. *Palaeoecology of Africa* 21:269–282.
Meadows, M.E. and J.M. Sugden 1991a The application of multiple discriminant-analysis to the reconstruction of the vegetation history of fynbos, southern Africa. *Grana* 30(2):325–336.
Meadows, M.E. and J.M. Sugden 1991b A vegetation history of the last 14,000 years on the Cederberg, southwestern Cape Province. *South African Journal of Science* 87(1-2):34–43.
Meadows, M.E. and J.M. Sugden 1993 The late Quaternary palaeoecology of a floristic kingdom: the southwestern Cape, South Africa. *Palaeogeography, Palaeoclimatology, Palaeoecology* 101(3-4):271–281.
Meadows, M.E., A.J. Baxter and J. Parkington 1996 Late Holocene environments at Verlorenvlei, Western Cape Province, South Africa. *Quaternary International* 33:81–95.
Miller, C.E., P. Goldberg and F. Berna 2013 Geoarchaeological investigations at Diepkloof rock shelter, Western Cape, South Africa. *Journal of Archaeological Science* 40(9):3432–3452.

Mitchell, P. 2002 *The archaeology of southern Africa*. Cambridge: Cambridge University Press.
Mitchell, P. 2008 Developing the archaeology of marine isotope stage 3. *Goodwin Series* 10:52–65.
Monge, G., F.J. Jimenez-Espejo, A. García-Alix, F. Martínez-Ruiz, N. Mattielli, C. Finlayson, N. Ohkouchi, M.C. Sánchez, J.M.B. De Castro, R. Blasco and J. Rosell 2015 Earliest evidence of pollution by heavy metals in archaeological sites. *Scientific reports* 5(1):1–9.
Monteath, T.L. 2001 *A History of South Africa*. London: Yale University Press.
Murray, A.S. and A.G. Wintle 2000 Luminescence dating of quartz using an improved single-aliquot regenerative-dose protocol. *Radiation measurements* 32(1):57–73.
Oonk, S., C.P. Slomp and D.J. Huisman 2009 Geochemistry as an aid in archaeological prospection and site interpretation: current issues and research directions. *Archaeological Prospection* 16(1):35–51.
Parkington, J., C. Cartwright, R.M. Cowling, A. Baxter and M. Meadows 2000 Palaeovegetation at the Last Glacial Maximum in the Western Cape, South Africa: wood charcoal and pollen evidence from Elands Bay Cave. *South African Journal of Science* 96(11–12):543–546.
Phillips, N., I. Moffat, A. Mackay and B.G. Jones 2023 The Sedimentary Context of Open-Air Archaeology: A Case Study in the Western Cape's Doring River Valley, South Africa. *Soil systems* 7(1):1–45.
Porraz, G. C., Tribolo, P. Schmidt, J.E. Parkington, M. Igreja, V.C. Schmid, N. Mercier, C.C. Cartwright, C.E. Miller, N.J. Conard and A. Charrié-Duhaut 2016 Update on the 2011 excavation at Elands Bay Cave (South Africa) and the Verlorenvlei stone age. *Southern African Humanities* 29(1):33–68.
Pye, K. and S.J. Blott 2004 Particle size analysis of sediments, soils and related particulate materials for forensic purposes using laser granulometry. *Forensic Science International* 144(1):19–27.
Reading, H.G. (ed.) 2009 *Sedimentary environments: processes, facies and stratigraphy*. Oxford: John Wiley & Sons.
Reidsma, F.H., I. Sifogeorgaki, A. Dinckal, H. Huisman, M.J. Sier, B. van Os and G.L. Dusseldor 2021 Making the invisible stratigraphy visible: a grid-based, multi-proxy geoarchaeological study of Umhlatuzana Rockshelter, South Africa. *Frontiers in Earth Science* 9:1–21
Reitz E.J. and M.L. Shackley 2012 *Environmental Archaeology*. New York: Springer.
Reynard, J.P. 2021 Paradise lost: large mammal remains as a proxy for environmental change from MIS 6 to the Holocene in southern Africa. *South African Journal of Geology* 124(4):1055–1072.
Schmidt, P. and A. Högberg 2018 Heat treatment in the still Bay-A case study on Hollow Rock Shelter, South Africa. *Journal of Archaeological Science* 21:712–720.
Schmidt, P. and A. Mackay 2016 Why was silcrete heat-treated in the Middle Stone Age? An early transformative technology in the context of raw material use at Mertenhof Rock Shelter, South Africa. *PLoS ONE* 11(2):1–16.
Schmidt, P., D. Stynder, N.J. Conard and J.E. Parkington 2020 When was silcrete heat treatment invented in South Africa? *Palgrave Communications 6*(1):1–10.
Schulte, E. E. and B. G Hopkins 1996 Estimation of Soil Organic Matter by Weight Loss-On-Ignition. In F. R. Magdoff, M. A. Tabatabai and E. A. Hanlon Jr. (eds), *Soil Organic Matter: Analysis and Interpretation*, pp.21–31. Soil Science Society of America 46. Madison: SSSA Special Publication.
Scott, L. and S. Woodborne 2007a Vegetation history inferred from pollen in Late Quaternary faecal deposits (hyraceum) in the Cape winter-rain region and its bearing on past climates in South Africa. *Quaternary Science Review* 26(7–8):941–953.
Scott, L. and S. Woodborne 2007b Pollen analysis and dating of Late Quaternary faecal deposits (hyraceum) in the Cederberg, Western Cape, South Africa. *Review of Palaeobotany and Palynology* 144(3–4):123–134.

Sealy, J. 2009 Modern behaviour in ancient South Africans: evidence for the heat treatment of stones in the Middle Stone Age: news & views. *South African Journal of Science* 105(9):323–324.
Shahack-Gross, R. 2017 Archaeological formation theory and geoarchaeology: State-of-the-art in 2016. *Journal of Archaeological Science 79*:36–43.
Shaw, M., C.J. Ames, N. Phillips, S. Chambers, A. Dosseto, M. Douglas, R. Goble, Z. Jacobs, B. Jones, S. Lin, and M.A. Low 2019 The Doring River Archaeology Project: approaching the evolution of human land use patterns in the Western Cape, South Africa. *PaleoAnthropology* 400–422.
Sifogeorgaki, I., V. Klinkenberg, I. Esteban, M. Murungi, A.S. Carr, V.B. van den Brink, and G.L. Dusseldorp 2020 New excavations at Umhlatuzana Rockshelter, KwaZulu-Natal, South Africa: a stratigraphic and taphonomic evaluation. *African Archaeological Review* 37(4):551–578.
Smykatz-Kloss, W. 2012 *Differential thermal analysis: application and results in mineralogy* (Vol. 11). Berlin: Springer Science & Business Media.
Stager, J. C., P.A. Mayewski, J.W.C. White, B.M. Chase, F.H. Neumann, M.E. Meadows, C.D. King and J.E. Dixon 2012 Precipitation variability in the winter rainfall zone of South Africa during the last 1400 yr linked to the austral westerlies. *Climate of the Past* 8(3):877–887.
Stolarczyk, R.E. and P. Schmidt 2018 Is early silcrete heat treatment a new behavioural proxy in the Middle Stone Age? *PLoS One 13*(10):1–21.
Stuut, J.B.W., M.A. Prins, R.R. Schneider, G.J. Weltje, J.F. Jansen and G. Postma 2002 A 300-kyr record of aridity and wind strength in southwestern Africa: inferences from grain-size distributions of sediments on Walvis Ridge, SE Atlantic. *Marine Geology* 180(1-4):221–233.
Taylor, R. E. and O. Bar-Yosef 2014 *Radiocarbon Dating: An Archaeological Perspective*. New York: Routledge.
Thackeray, J.F. 2002 Palaeoenvironmental change and re-assessment of the age of Late Pleistocene deposits at Die Kelders cave, South Africa. *Journal of human evolution* 43(5):749–753.
Tite, M.S. 1972 The influence of geology on the magnetic susceptibility of soils on archaeological sites. *Archaeometry* 14(2):229–236.
Tite, M.S. and C. Mullins 1971 Enhancement of the magnetic susceptibility of soils on archaeological sites. *Archaeometry* 13(2):209–219.
Tribolo, C., N. Mercier, E. Douville, J.L. Joron, J.L. Reyss, D. Rufer, N. Cantin, Y. Lefrais, C.E. Miller, G. Porraz, J. Parkington, J.P. Rigaud and P.J. Texier 2013 OSL and TL dating of the Middle Stone Age sequence at Diepkloof Rock Shelter (South Africa): a clarification. *Journal of Archaeological Science* 40(9):3401–3411.
Valladas, H., L. Wadley, N. Mercier, L. Froget, C. Tribolo, J.L. Reyss, and J.L. Joron 2005 Thermoluminescence dating on burnt lithics from Middle Stone Age layers at Rose Cottage Cave. *South African Journal of Science* 101(3):169–174.
Valsecchi, V., B. M. Chase, J. A. Slingsby, A. S. Carr, L. J. Quick, M. E. Meadows, R. Cheddadi and P.J. Reimer 2013 A high resolution 15,600-year pollen and microcharcoal record from the Cederberg Mountains, South Africa. *Palaeogeography, Palaeoclimatology, Palaeoecology* 387:6–16.
Villa, P., S. Soriano, N. Teyssandier and S. Wurz 2010 The Howiesons Poort and MSA III at Klasies River main site, cave 1A. *Journal of Archaeological Science 37*(3):630–655.
Visher, G.S. 1969 Grain size distributions and depositional processes. *Journal of Sedimentary Research* 39(3):1074–1106.
Wadley, L. 2001 What is cultural modernity? A general view and a South African perspective from Rose Cottage Cave. *Cambridge archaeological journal* 11(2):201–221.

Waters, M.R. and D.D. Kuehn 1996 The geoarchaeology of place: The effect of geological processes on the preservation and interpretation of the archaeological record. *American Antiquity* 61(3):483–497.

Weldeab, S., J.B. Stuut, R.R. Schneider and W. Siebel 2013 Holocene climate variability in the winter rainfall zone of South Africa. *Climate of the Past 9*(5):2347-2364.

Wells, M.J. 1991 Introduced plants of the fynbos biome. In R. H. Groves and F. Di Castri (eds), *Biogeography of Mediterranean Invasions,* pp.115–129. Botanical Research Institute. Cambridge: Cambridge University Press.

Will, M., A. Mackay and N. Phillips 2015 Implications of Nubian-like core reduction systems in southern Africa for the identification of early modern human dispersals. *PLoS One* 10(6):1–21.

Williams, A.N., P. Veth, W. Steffen, S. Ulm, C.S. Turney, J.M. Reeves, S.J. Phipps, and M. Smith 2015 A continental narrative: Human settlement patterns and Australian climate change over the last 35,000 years. *Quaternary Science Reviews 123*:91–112.

Williams, M.P. 2017 Formation processes and context of complex stratigraphic features at the MSA archaeological sites of Pinnacle Point Site 5-6 and Mertenhof during MIS 3 in southern Africa. Honours degree of Bachelor of Science, School of Earth & Environmental Sciences, University of Wollongong, Wollongong.

Wurz, S. 1999 The Howiesons Poort backed artefacts from Klasies River: an argument for symbolic behaviour. *The South African Archaeological Bulletin* 54:38–50.